iScience

CellPress
OPEN ACCESS

Article

Quantitative Proteomics Identifies TCF1 as a Negative Regulator of *Foxp3* Expression in Conventional T Cells

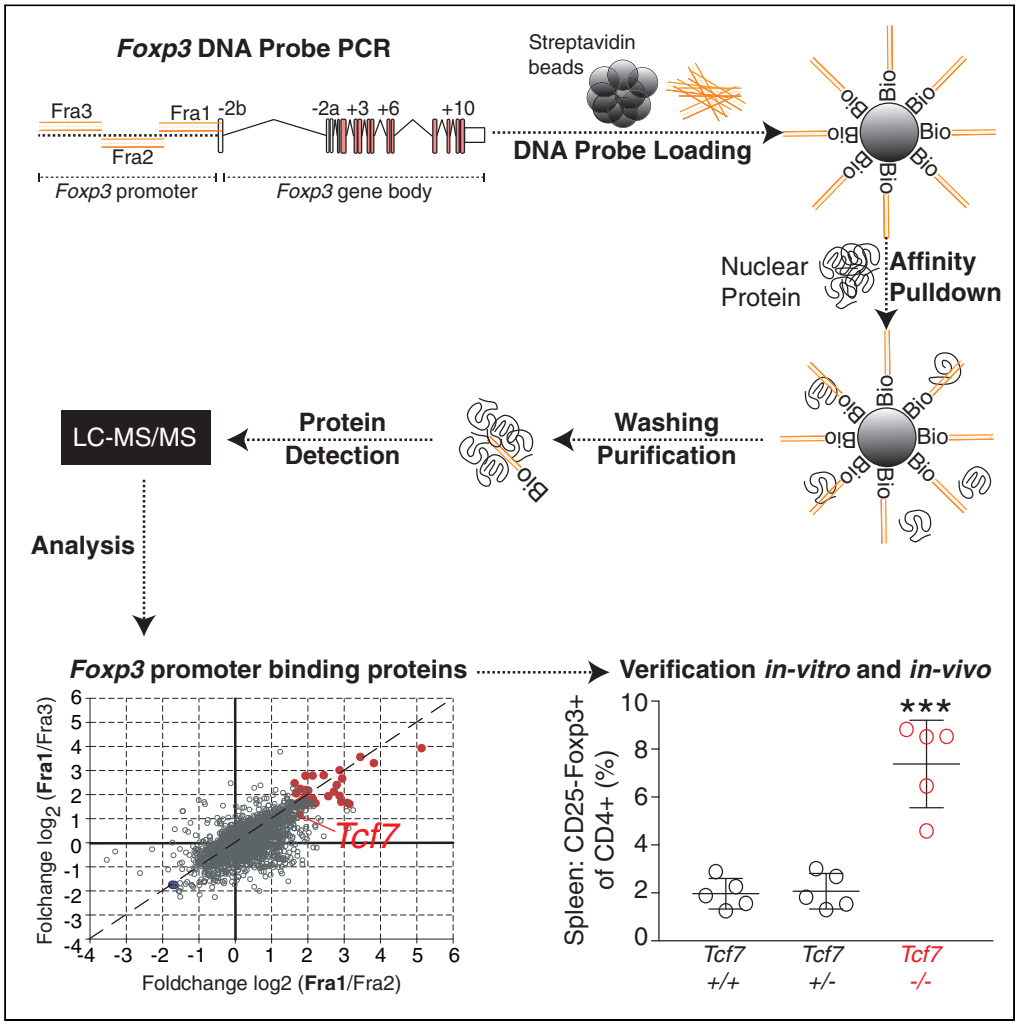

Michael Delacher, Melanie M. Barra, Yonatan Herzig, ..., Jakub Abramson, Jeroen Krijgsveld, Markus Feuerer

markus.feuerer@ukr.de

HIGHLIGHTS

Quantitative proteomics identifies proteins bound to the *Foxp3* gene promoter

Promoter-binding proteins are suppressing Foxp3 expression

TCF1-deficient animals have more Foxp3-expressing $CTLA4^{-}CD25^{-}CD4^{+}$ T cells

TCF1 suppresses Foxp3 expression in activated non-T_{reg} cells

Delacher et al., iScience *23*, 101127
May 22, 2020
https://doi.org/10.1016/j.isci.2020.101127

iScience

CellPress
OPEN ACCESS

Article

Quantitative Proteomics Identifies TCF1 as a Negative Regulator of *Foxp3* Expression in Conventional T Cells

Michael Delacher,[1,2,3] Melanie M. Barra,[3] Yonatan Herzig,[4] Katrin Eichelbaum,[5] Mahmoud-Reza Rafiee,[5] David M. Richards,[3] Ulrike Träger,[3] Ann-Cathrin Hofer,[3] Alexander Kazakov,[3] Kathrin L. Braband,[3] Marina Gonzalez,[3] Lukas Wöhrl,[2] Kathrin Schambeck,[2] Charles D. Imbusch,[6,7] Jakub Abramson,[4] Jeroen Krijgsveld,[5,8,9] and Markus Feuerer[1,2,3,10,*]

SUMMARY

Regulatory T cells are important regulators of the immune system and have versatile functions for the homeostasis and repair of tissues. They express the forkhead box transcription factor Foxp3 as a lineage-defining protein. Negative regulators of Foxp3 expression are not well understood. Here, we generated double-stranded DNA probes complementary to the *Foxp3* promoter sequence and performed a pull-down with nuclear protein *in vitro*, followed by elution of bound proteins and quantitative mass spectrometry. Of the *Foxp3*-promoter-binding transcription factors identified with this approach, one was T cell factor 1 (TCF1). Using viral over-expression, we identified TCF1 as a repressor of Foxp3 expression. In TCF1-deficient animals, increased levels of Foxp3^{intermediate}CD25^{negative} T cells were identified. CRISPR-Cas9 knockout studies in primary human and mouse conventional CD4 T (T_{conv}) cells revealed that TCF1 protects T_{conv} cells from inadvertent Foxp3 expression. Our data implicate a role of TCF1 in suppressing Foxp3 expression in activated T cells.

INTRODUCTION

Foxp3 is the master transcription factor (TF) for regulatory T (T_{reg}) cells, and its absence leads to catastrophic autoimmune events in mice (Scurfy phenotype; Brunkow et al., 2001; Fontenot et al., 2003; Wildin et al., 2001) and humans (IPEX or immune dysregulation, polyendocrinopathy, enteropathy, X-linked syndrome; Bennett et al., 2001). Foxp3 expression in concert with a specific epigenetic landscape induced in the thymus defines T_{reg} cells (Ohkura et al., 2012). A subset of T_{reg} cells can acquire epigenetic and transcriptional profiles defining their tissue adaptation (Delacher et al., 2017, 2019, 2020; Schmidl et al., 2018).

The *Foxp3* gene is located on the X chromosome. It contains 14 exons, three of which are not translated (-2a, -2b, and −1). The promoter with TATA box, GC box, and CAAT box is located just upstream of the transcription start site (TSS). When comparing the sequence homology between mouse and human *Foxp3* genetic code, a high degree of conservation can be appreciated for the coding exons, three regions in non-coding introns, and the promoter itself (Andersen et al., 2012; Janson et al., 2008; Sadlon et al., 2010; Xie et al., 2015). The three distinct conserved regions within the intronic sequences of the *Foxp3* gene were determined as conserved non-coding sequences 1, 2, and 3 (CNS1-3). Each CNS region has a distinct function in the initiation or stabilization of *Foxp3* gene expression, just like the core *Foxp3* promoter (Delacher et al., 2014; Rudensky, 2011). A fourth conserved region outside the Foxp3 gene, named CNS0, has recently been described (Kitagawa et al., 2017).

CNS0 contains T_{reg}-specific super-enhancers crucial for T_{reg} cell lineage specification in the thymus (Kitagawa et al., 2017). CNS1 is an important transforming growth factor (TGF)-β-sensitive enhancer region for the induction of peripherally induced T_{reg} (pT_{reg}) from Foxp3$^-$ conventional CD4 T (T_{conv}) cells *in vivo* and for the *in vitro* conversion of T_{reg} cells from T_{conv}. CNS1 is not relevant for thymic T_{reg} cell generation (Josefowicz et al., 2012; Schlenner et al., 2012; Tone et al., 2008). The CNS2 region contains a high number of CpG sites, becomes demethylated in the thymus, and has an important role to stabilize Foxp3 expression

[1]Chair for Immunology, Regensburg University, Franz-Josef-Strauss-Allee 11, 93053 Regensburg, Germany

[2]Regensburg Center for Interventional Immunology (RCI), Franz-Josef-Strauss-Allee 11, 93053 Regensburg, Germany

[3]Immune Tolerance Group, Tumor Immunology Program, German Cancer Research Center (DKFZ), Im Neuenheimer Feld 280, 69120 Heidelberg, Germany

[4]Department of Immunology, Weizmann Institute of Science, 234 Herzl Street, 76100 Rehovot, Israel

[5]European Molecular Biology Laboratory, Meyerhofstraße 1, 69117 Heidelberg, Germany

[6]Faculty of Biosciences, Heidelberg University, Im Neuenheimer Feld 234, 69120 Heidelberg, Germany

[7]Division of Applied Bioinformatics, German Cancer Research Center (DKFZ), Im Neuenheimer Feld 581, 69120 Heidelberg, Germany

[8]Proteomics of Stem Cells and Cancer, German Cancer Research Center (DKFZ), Im Neuenheimer Feld 581, 69120 Heidelberg, Germany

[9]Medical Faculty, Heidelberg University, Im Neuenheimer Feld 672, 69120 Heidelberg, Germany

[10]Lead Contact

*Correspondence: markus.feuerer@ukr.de

https://doi.org/10.1016/j.isci.2020.101127

(Delacher et al., 2017; Floess et al., 2007; Zheng et al., 2010). In addition, some factors bind this region to stabilize the demethylated phenotype (Kim and Leonard, 2007; Mouly et al., 2010). The CNS3 is a pioneer element required for efficient induction of *Foxp3* transcription (Schuster et al., 2012; Zheng et al., 2010).

The precise location of the *Foxp3* promoter and the true TSS were identified in a study utilizing rapid amplification of 5′ ends, proving that the core promoter is indeed the area where DNA-dependent RNA transcription of *Foxp3* pre-mRNA begins (Tone et al., 2008).

Several studies identified Nfat (nuclear factor of activated T cells) binding to the *Foxp3* promoter, and mutations in the *Nfat*-binding sites or deficiency in calcium sensing disrupted its activity (Mantel et al., 2006; Oh-Hora et al., 2013; Tone et al., 2008). In addition, a set of Forkhead Box proteins (Foxo1 and Foxo3a) bind the *Foxp3* promoter as part of the PI3K-Akt-mTOR pathway, and their specific deletion caused multifocal inflammatory disorder (Harada et al., 2010; Ouyang et al., 2010). Stat5 (signal transducer of activated T cells 5) has also been detected at the *Foxp3* gene promoter, and its selective deletion prevents T_{reg} cell development (Burchill et al., 2007; Yao et al., 2007). Another example of direct *Foxp3* promoter regulation is the study of nuclear receptor subfamily members: mice devoid of all three subfamily members (Nr4a1, Nr4a2, Nr4a3) cannot produce T_{reg} cells and die of systemic autoimmunity (Sekiya et al., 2011, 2013). Several studies identified the c-Rel enhanceosome complex (Ruan et al., 2009) as well as Runx proteins (Bruno et al., 2009; Klunker et al., 2009) at the *Foxp3* promoter. Finally, *Foxp3*-promoter-binding partners have been identified in the E2A-Id3 signaling axis and have been shown to influence Foxp3 expression (Wang et al., 2011; Wohlfert et al., 2011).

These studies have identified an impressive set of Foxp3-inducing factors. However, much less is known about Foxp3-repressive factors required to protect Foxp3-negative T_{conv} cells from unwanted Foxp3 expression, e.g., as a by-product of T cell activation.

We wanted to identify *Foxp3*-promoter-binding proteins in an unbiased way using quantitative mass spectrometry (Mittler et al., 2009). With this approach, we identified several binding partners to the *Foxp3* promoter region with repressive effect on the *Foxp3* promoter. One of those Foxp3-promoter-suppressive factors was T cell factor 1 (TCF1), which we followed up by Luciferase-based-binding studies, by overexpression and deletion studies in primary T cells, and by the analysis of a TCF1-deficient mouse strain. Our data point toward a specific role of TCF1 to suppress Foxp3 expression in activated non-T_{reg} cells.

RESULTS

Quantitative Proteomics Identifies *Foxp3*-Promoter-Binding Factors

We visualized the conservation of *Foxp3* genetic code between mouse and human and superimposed the *Foxp3* gene structure to identify target regions for protein binding identification (Figure 1A). We could observe that the *Foxp3* gene promoter, at least in its very proximal 500 bp, was highly conserved between mouse and human. In addition, the proximal promoter was demethylated in both T_{reg} and T_{conv} cells, whereas intron-1 was specifically demethylated only in T_{reg} cells. We generated three 500-bp DNA probes complementary to the *Foxp3* promoter region: *Foxp3*-Fra1, starting from the *Foxp3* TSS and extending 500 bp upstream into the promoter region (−500); *Foxp3*-Fra2, extending −500 bp to −1000 bp into the *Foxp3* promoter; and *Foxp3*-Fra3, extending from −1000 bp to −1500 bp into the distal *Foxp3* promoter region (Figure 1A). All three fragments were generated with biotin-labeled primers to use them as probes for an *in vitro* pull-down followed by mass spectrometry (Mittler et al., 2009) (Figure 1B). First, streptavidin beads were linked to biotinylated *Foxp3* promoter Fra1, Fra2, or Fra3 probes, followed by incubation with nuclear proteins isolated from EL4 T cells. We used EL4 T cells as a Foxp3-negative cell line to study potential repressive elements binding to the Foxp3 promoter. Unbound protein was washed off, and beads including attached proteins were isolated in a magnetic field. Protein was eluted from the beads and purified, digested, labeled with stable isotopes, fractionated, and finally subjected to nano-liquid chromatography-mass spectrometry analysis allowing the quantitative detection of peptides bound to each DNA probe.

The experiment was done in two replicates, yielding more than 2,500 proteins bound to each DNA probe (Figure 2A). Of the around 2,400 proteins that could be quantified with each probe, 43, 23, and 23 were differentially bound to Fra1, Fra2, and Fra3, respectively (fold-change $\log_2$>3 compared with the other two probes, false discovery rate [FDR] <1%). All binding partners to Fra1 are displayed in a dot plot for relative binding as well as a volcano plot to visualize selection based on statistics ($p < 0.01$) and fold-change

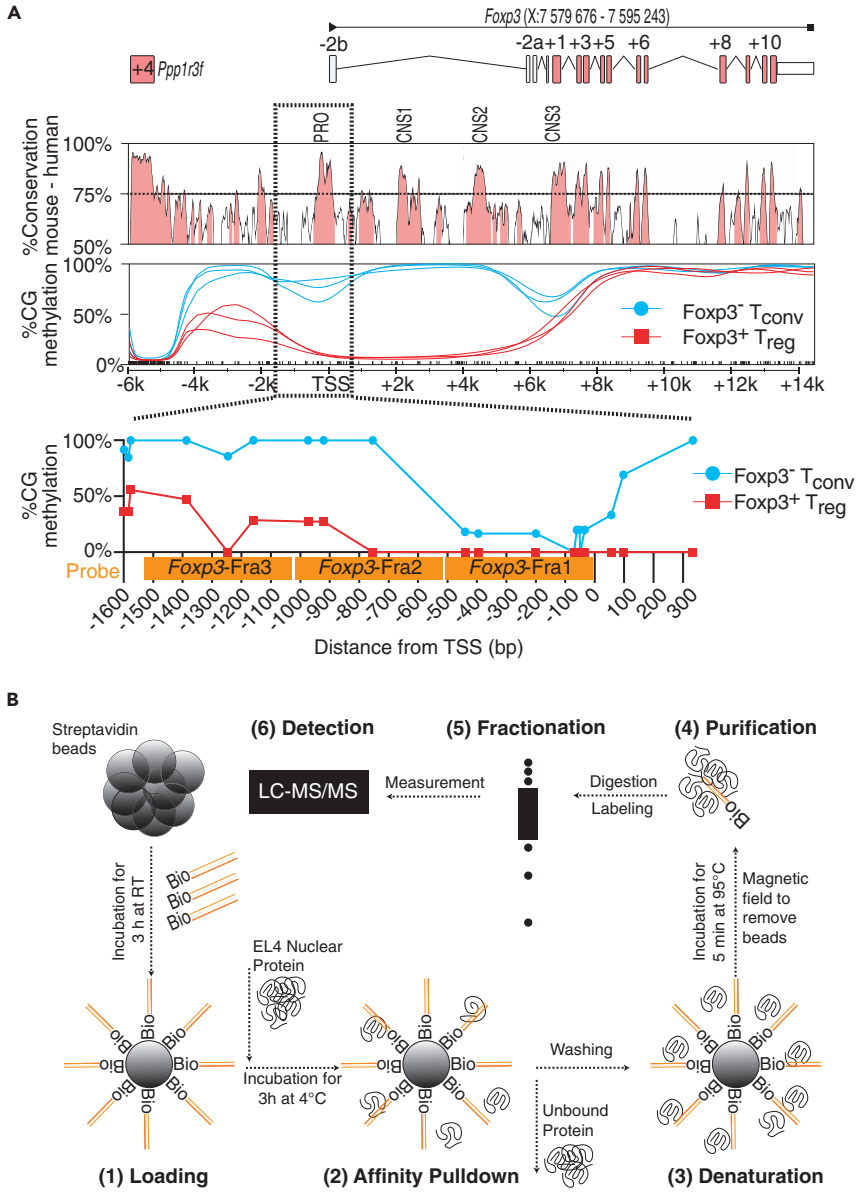

Figure 1. Quantitative Proteomics of the *Foxp3* Promoter

(A) Conservation between mouse (CCDS29965) and human (CCDS14323) *Foxp3* genetic code. The y axis indicates conservation between genetic code in %, and the x axis indicates genomic location. Histogram generated with Vista (Mayor et al., 2000). Labels PRO (promoter) and CNS (conserved non-coding sequence) on top. Below, CG methylation of the *Foxp3* gene (X:7,579,676-7,595,243) with three replicate T_{reg} and T_{conv} cells, data published previously (Delacher et al., 2017). Beneath histograms, magnification of the *Foxp3* promoter region from −1600 bp to +300 bp relative to the Foxp3 TSS with methylation levels of individual CGs. Probes for proteomics are labeled in orange.

(B) Overview of the quantitative proteomics procedure. First, beads are loaded with biotinylated *Foxp3*-Fra1, *Foxp3*-Fra2, or *Foxp3*-Fra3 probes (Loading [1]). Then, loaded beads are incubated with nuclear proteins and purified in magnetic field (Affinity pull-down [2]). Proteins are denatured (Denaturation [3]) and purified (Purification [4]), followed by Fractionation (5) and Detection (6) via nano-liquid chromatography-tandem mass spectrometry (LC-MS/MS).

(log_2>3, Figure 2B). Proteins with positive binding values (in the comparison Fra1 versus Fra2 and Fra1 versus Fra3) were identified and labeled in red, whereas proteins with negative binding values (e.g., not binding to Fra1, but to Fra2 or Fra3) were labeled in blue. Proteins that bound equally to both fragments were labeled in gray. A heatmap with differential binding values for all selected proteins for Fra1 clarifies selective binding patterns of all candidate factors: out of the 43 proteins that bound differentially to Fra1

A

Foxp3 promoter binding partner to:	Fra1	Fra2	Fra3
Proteins Replicate 1	2658	2645	2648
Proteins Replicate 2	2723	2727	2727
Quantified Proteins	2349	2343	2348
FDR 1%, foldchange log2>2	99	52	57
FDR 1%, foldchange log2>3	**43**	**23**	**12**
FDR 1%, foldchange log2>3, positive binding	41	05	05
FDR 1%, foldchange log2>3, negative binding	02	18	07

B

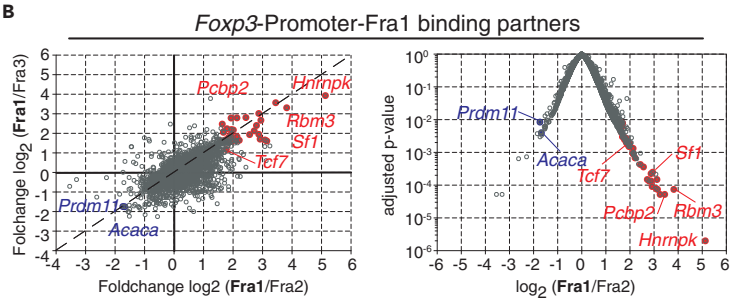

C

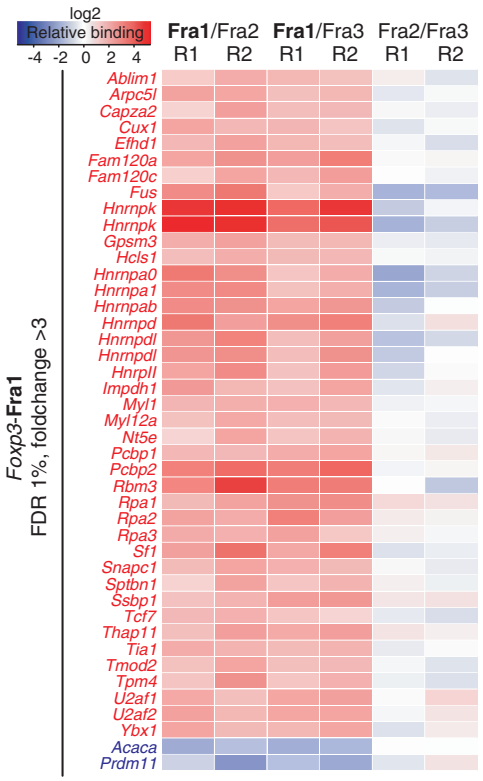

D

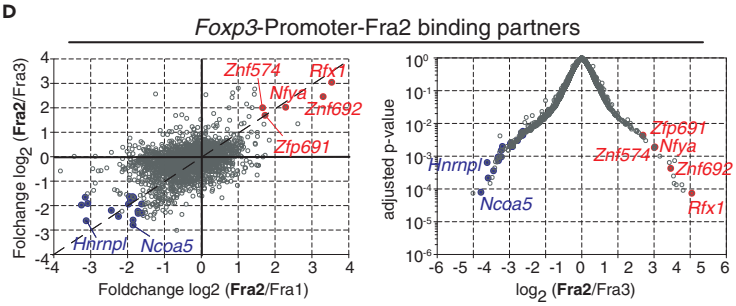

E

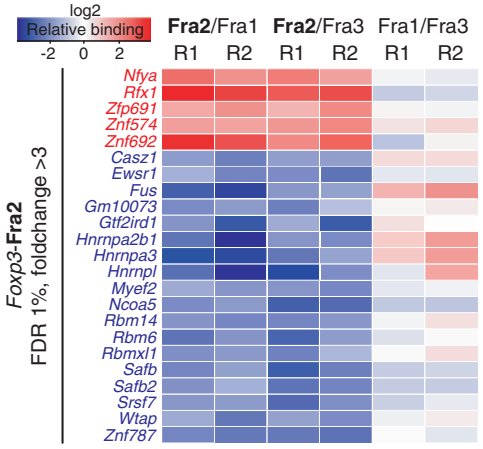

F

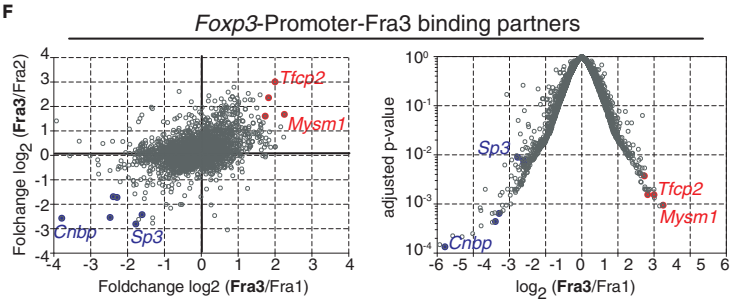

G

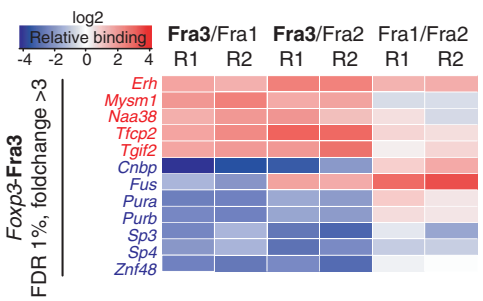

Figure 2. Proteins Identified at the *Foxp3* Promoter

(A) Results of quantitative proteomics of the *Foxp3* promoter with two replicates; FDR, false discovery rate. Bold numbers indicate differential binding partners to the respective fragment (FDR 1%, fold-change log2>3). Red numbers indicate positive binding partners, blue numbers negative binding partners to the respective fragment.

(B) Results for *Foxp3*-Fra1. Left dot plots illustrate all detected proteins with relative binding values to Fra1 versus Fra3 (y axis) and Fra1 versus Fra2 (x axis). Right graph, volcano plot with Fra1 versus Fra2 relative binding (x axis) versus adjusted p value (y axis). Key genes are highlighted. Positive and negative binding partners (FDR 1%, fold-change log2>3) are highlighted.

(C) Heatmap illustrating relative binding of Fra1 candidates to Fra1, Fra2, and Fra3 (FDR 1%, fold-change log2>3).

(D) Results for *Foxp3*-Fra2. Left dot plots illustrate all detected proteins with relative binding values to Fra2 versus Fra3 (y axis) and Fra2 versus Fra1 (x axis). Right graph, volcano plot with Fra2 versus Fra3 relative binding (x axis) versus adjusted p value (y axis). Key genes are highlighted. Positive and negative binding partners (FDR 1%, fold-change log2>3) are highlighted.

(E) Heatmap illustrating relative binding of Fra2 candidates to Fra1, Fra2, and Fra3 (FDR 1%, fold-change log2>3).

(F) Results for *Foxp3*-Fra3. Left dot plots illustrate all detected proteins with relative binding values to Fra3 versus Fra2 (y axis) and Fra3 versus Fra1 (x axis). Right graph, volcano plot with Fra3 versus Fra1 relative binding (x axis) versus adjusted p value (y axis). Key genes are highlighted. Positive and negative binding partners (FDR 1%, fold-change log2>3) are highlighted.

(G) Heatmap illustrating relative binding of Fra3 candidates to Fra1, Fra2, and Fra3 (FDR 1%, fold-change log2>3). Data are representative of two independent experiments.

versus Fra2 and Fra 1 versus Fra3, 41 were enriched on Fra1, being potential candidates for downstream testing. Two proteins bound strongly to Fra2 or Fra3, but not Fra1, and were excluded.

To identify candidates' binding to Fra2, we again display dot plot and heatmap (Figures 2D and 2E). Of the 23 proteins that bound differentially to Fra2 versus Fra1 and Fra2 versus Fra3, five bound specifically to Fra2. All other candidates bound strongly to Fra1 or Fra3 and were excluded for downstream testing. For Fra3, 5 of 12 proteins were enriched on the Fra3-binding sites and used to select candidate factors (Figures 2F and 2G). Therefore, in summary, we identified 41 factors bound to Fra1, 5 factors bound to Fra2, and 5 factors bound to Fra3.

Foxp3-Promoter-Binding TFs Down-modulate *Foxp3* Promoter Activity *In Vitro*

For our proteomics experiments, we used nuclear protein derived from a T cell line. To avoid cell line artifacts, we measured expression levels of some candidate factors in primary murine T_{reg} and T_{conv} cells as well as in EL4 and RMA mouse T cell lines by real-time PCR. Most factors were expressed in primary T_{reg} and T_{conv} cells and cell lines (Figure S1A). In addition, we isolated T_{reg} and T_{conv} cells from human peripheral blood and measured the expression of some candidate factors by real-time PCR and included three T cell lines (Jurkat, CEM, and BE, Figure S1B). As seen for mouse, most factors were also expressed in primary human T cells.

To explore the function of candidate proteins with Luciferase reporter vectors, we cloned nine factors from Fra1, five factors from Fra2, and three factors from Fra3 into eukaryotic production vectors. All vectors were sequenced to confirm plasmid identity and sequence integrity, and we verified plasmid stability by gel electrophoresis (Figure S1C). In addition, we confirmed transgene expression for selected transgenes by western blot (Figure S2A) and confirmed plasmid identity (Figure S2B). Using a eukaryotic vector expression system, we transfected the respective candidate factors, a *Foxp3* promoter vector with *Luciferase* reporter (Sekiya et al., 2011) and a *beta-galactosidase* transfection and normalization control vector into HEK293 cells (Figure S3A). After 2 days, we measured Luciferase and β-galactosidase enzymatic activity. To cross-validate our dataset, we used a Luciferase basic vector without promoter, a full *Foxp3* promoter Luciferase vector (containing 3,500 bp of the *Foxp3* promoter, location X:7,576,145- X:7,589,866 [10190 bp]), and short 500-bp *Foxp3* promoter Luciferase vectors (Figure S3B). These short fragments were identical to the probes used for quantitative proteomics (Figure 1A). Using this system, we first measured light induction by GFP (negative control) and Nr4a1 (positive control). As expected, GFP expression did not induce activity together with the basic vector, the full *Foxp3* promoter vector, or a vector containing only *Foxp3* Fra1 (Figure S3C, left). In contrast to this, the Nr4a1 transgene induced significant activity at the full *Foxp3* promoter vector, but not in the Fra1 or the basic vector (Figure S3C, right). Nr4a1 binding to the *Foxp3* gene has already been described in the literature (Sekiya et al., 2011, 2013). Next, we tested the candidates identified with our screening method with this assay. None of the factors induced *Foxp3* promoter Luciferase activity in the short (Fra1, Fra2, Fra3) or the full *Foxp3* promoter vector. In contrast to this, some of the factors such as Sf1 (splicing factor 1), Znf574 (zinc finger protein 574), Rfx1 (regulatory factor X,1), or Naa38 (Nα-acetyltransferase 38, NatC auxiliary subunit) showed a significant down-modulation of Luciferase activity at one of the *Foxp3* promoter vectors (Figures S3D–S3F). Taken together, our Luciferase screens demonstrate that some of our candidate factors showed significant repressive activity and down-modulated basic *Foxp3* promoter activity.

Candidate Factors Overrule Activation-Induced *Foxp3* Promoter Activity

In the previous experiments, we identified *Foxp3*-promoter-binding TFs and observed that they down-modulated basic *Foxp3* promoter activity. *Foxp3* promoter signaling can also be induced by T cell receptor (TCR) stimulation (Mantel et al., 2006; Oh-Hora et al., 2013; Tone et al., 2008). Therefore, we established a system where Jurkat T cells were electroporated with a *Foxp3* promoter vector, a eukaryotic production vector carrying the candidate transgene, and a *Renilla* normalization and transfection control vector (Figure S4A). After 24 h, TCR signaling was mimicked by phorbol myristate acetate (PMA)/Ionomycin (PMA/IM) stimulation. After 24 h, Luciferase and Renilla activities were measured by luminescence, as before. When comparing results for the basic vector without any promoter sequence and the *Foxp3* promoter vector, PMA/IM stimulation increased *Foxp3* promoter activity by about 10-fold (Figure S4B). We tested several candidate transgenes with this system. No changes were observed when using the basic Luciferase vector. In contrast to this, PMA/IM stimulation induced activity with the *Foxp3* promoter vector. Interestingly, some of the factors such as Pcbp1, Pcbp2, and Thap11 significantly down-regulated Luciferase activity with the *Foxp3* promoter, but not with the basic vector without a promoter sequence (Figures S3C–S3E). These data indicate that certain TCR signals induced by treatment of cells with PMA/IM can be suppressed by individual candidate factors, providing additional evidence of their *Foxp3*-suppressive nature.

Candidate TF Expression Levels in Primary T_{reg} and T_{conv} Cells Identifies TCF1

In the previous experiments, we confirmed the *Foxp3*-suppressive nature of multiple TFs with our proteomics approach. Now, to select a candidate TF for further evaluation, we used a funnel approach using published proteome datasets. Ideally, a candidate TF should be up-regulated in Foxp3-negative T_{conv} cells. Two recent studies investigated the differential proteome between murine T_{reg} and T_{conv} cells (Barra et al., 2015a) and human T_{reg} and T_{conv} cells (Cuadrado et al., 2018). We extracted both datasets and identified our target *Foxp3*-promoter-binding factors. When comparing the 5,129 proteins identified in bulk murine $Foxp3^+$ T_{reg} versus $Foxp3^-$ T_{conv}, we could map 162 of 209 *Foxp3*-promoter-binding factors (fold-change log2>2, FDR < 1%) to this dataset (Figure 3A). One example for a highly significant T_{conv}-over-expressed factor that also binds the *Foxp3* promoter in our study is TCF1. When using the dataset derived from human effector T_{conv} versus effector T_{reg} cells, we could map 138 proteins of 209 *Foxp3*-promoter-binding factors (Figure 3B). Again, TCF1 was detected as T_{conv}-specific over-expressed factor. Therefore, human and mouse T_{reg}/T_{conv} proteomic datasets indicate that TCF1, a candidate protein identified with our *Foxp3*-promoter-binding screening (Figures 2B and 2C), is also a differentially expressed TF in Foxp3-positive versus Foxp3-negative T cells. To further validate this, we stained $CD4^+Foxp3^-$ T_{conv} cells, $CD4^+Foxp3^+$ T_{reg} cells, and $CD4^-CD8^+$ cytotoxic T cells and measured TCF1 expression levels by flow cytometry. As a control, we used $Tcf7^{-/-}$ animals ($Tcf7^{-/-}$ animals lack the TCF1 protein) (Verbeek et al., 1995). In spleen, T_{conv} and CD8 T cells expressed elevated TCF1 levels, whereas T_{reg} cells had significantly lower expression values (Figure 3C). To test if TCF1 has a repressive function on the *Foxp3* promoter, we used PMA/IM-stimulated Jurkat cells and electroporated a *Tcf7* eukaryotic production vector (Figure 3D). Interestingly, the TCF1 overexpression showed significant capacity to down-modulate the activity of the *Foxp3* promoter, but not the basic promoter (Figure 3E). In summary, we showed that TCF1 is expressed more specifically in Foxp3-negative T_{conv} cells and that the TCF1 protein has the capacity to down-modulate *Foxp3* promoter activity, similar to other proteins identified by quantitative proteomics of the *Foxp3* promoter.

TCF1 Overexpression Impairs Foxp3 Induction

To validate the impact of TCF1 on *Foxp3* gene expression in mature T_{reg} cells, we transduced primary T_{reg} cells with a *Tcf7*-MSCV retrovirus, with CD90.1 as a reporter for viral transduction and transgene expression (Figure 4A). The percentage of Foxp3 expression remained high in both *Tcf7*- and control-virus-transduced T_{reg} cells and was not affected by TCF1 protein production. In contrast to this, the Foxp3 median fluorescence intensity (MFI) was significantly reduced in TCF1-overexpressing T_{reg} cells, indicating that TCF1 can influence *Foxp3* gene expression in mature T_{reg} cells (Figure 4B). In line with this finding, we wanted to test the influence of TCF1 on the *de novo* induction of Foxp3 expression. To do so, we over-expressed TCF1 or a control protein in T_{conv} cells under TGF-β differentiation conditions, followed by measurement of intracellular Foxp3 levels (Figure 4C). Indeed, upon over-expressing TCF1, Foxp3 levels were reduced in percent and MFI, indicating that TCF1 also restrains Foxp3 induction (Figure 4D). Our data indicate that TCF1 impairs Foxp3 induction and maintenance *in vitro*.

TCF1-Deficient Animals Have More $CD25^{neg}Foxp3^{int}$ T cells in the Periphery

To validate the relevance of TCF1 *in vivo*, we analyzed $Tcf7^{-/-}$ animals (Verbeek et al., 1995). First, we measured the frequency of $CD4^+CD25^+Foxp3^+$ T_{reg} cells in lymph node and spleen of $Tcf7^{-/-}$, $Tcf7^{+/-}$, and $Tcf7^{+/+}$

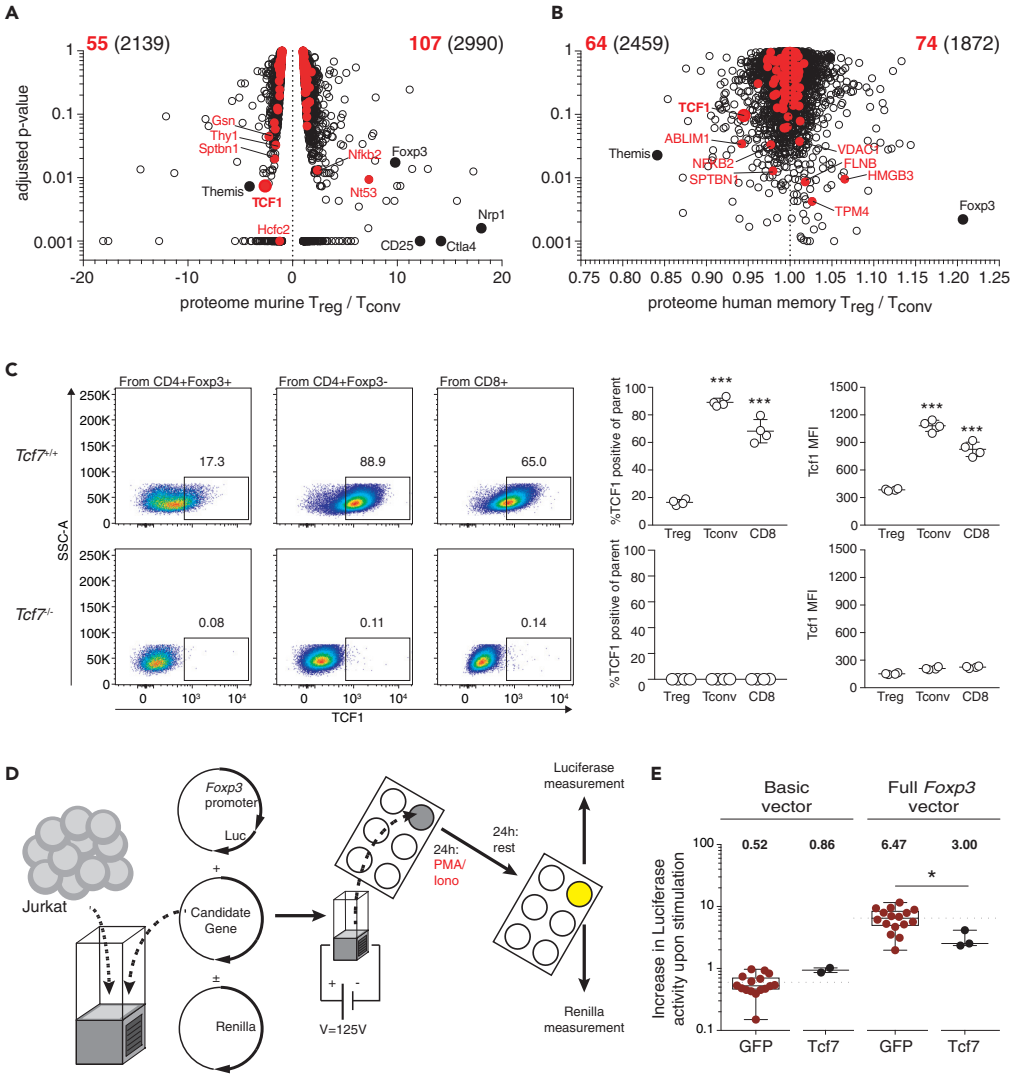

Figure 3. Funnel Approach Identifies TCF1 as Foxp3-Regulating TF

(A) 5,129 proteins comparing bulk murine Foxp3$^+$ T_{reg} versus Foxp3$^-$ T_{conv} were extracted from Barra et al. (2015a) and compared with our proteomics dataset. Data are displayed in a volcano plot with adjusted p value (y axis) versus protein expression T_{reg} versus T_{conv} (x axis). 162 out of 209 *Foxp3*-promoter-binding factors (fold-change log2>2, FDR<1%) were mapped to this dataset and highlighted in red. Key TF labeled.

(B) 4,331 proteins comparing bulk human effector T_{reg} versus T_{conv} were extracted from Cuadrado et al. (2018) and compared with our proteomics dataset. Data are displayed in a volcano plot with adjusted p value (y axis) versus protein expression T_{reg} versus T_{conv} (x axis). 138 of 209 *Foxp3*-promoter-binding factors (fold-change log2>2, FDR<1%) were mapped to this dataset and highlighted in red. Key TF labeled.

(C) Analysis of TCF1 protein expression in *Tcf7*$^{+/+}$ animals (top) and *Tcf7*$^{-/-}$ animals (below). Left, dot plots illustrating TCF1 expression in T_{reg} cells (CD8$^-$CD4$^+$Foxp3$^+$), T_{conv} cells (CD8$^-$CD4$^+$Foxp3$^-$), and CD8 T cells (CD4$^-$CD8$^+$). Right, statistical analysis across replicates (n = 4, one-way ANOVA, error bars = standard deviation, ***p < 0.001).

(D) Experiment overview: 2,000,000 Jurkat cells were electroporated with a Renilla normalization vector, *Foxp3*-Luciferase reporter vector, and a eukaryotic expression vector containing the transgene of interest; 24 h after electroporation, cells were stimulated with PMA/Ionomycin, and 20 h after stimulation, cells were lysed and Renilla as well as Luciferase enzyme activities were measured on a luminometer with automated injection of substrates.

(E) Jurkat cells were electroporated with a Renilla normalization vector, *Foxp3*-Luciferase reporter vector, and a *GFP* or *TCF1* eukaryotic expression vector. Statistical testing with unpaired t test (n = 3–16, *p < 0.05). Data are derived from literature or two or more independent experiments.

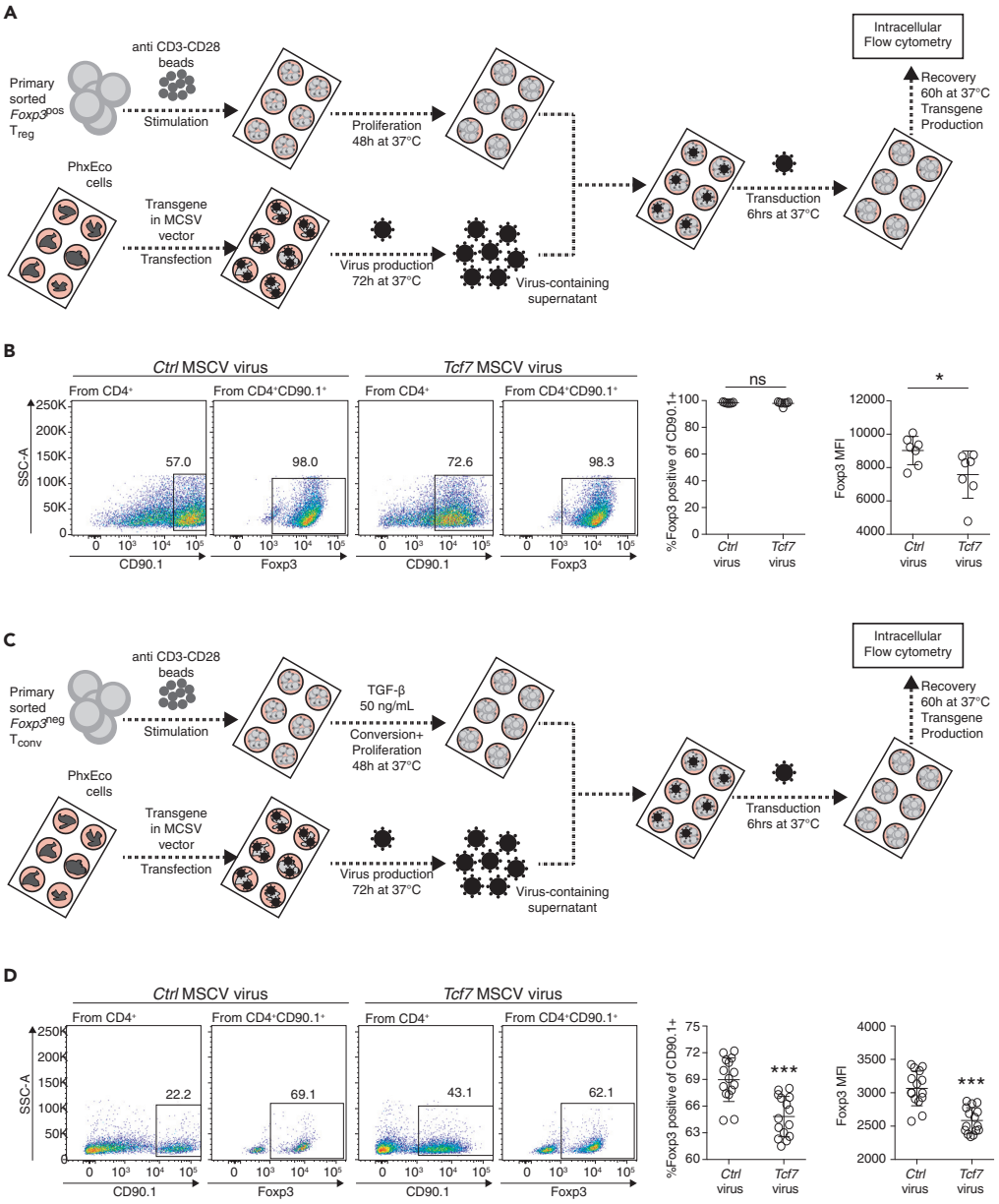

Figure 4. Effect of TCF1 Overexpression on Thymus-Derived thymic T_{reg} or *In Vitro* Converted iT_{reg} Cells

(A) Experiment overview: Primary murine $CD4^+CD25^+$*Foxp3*$(GFP)^+$ T_{reg} cells were purified by fluorescence-activated cell sorting (FACS), stimulated with anti-CD3/28 beads plus interleukin-2, and expanded for 48 h at 37°C. Then, virus-containing supernatant derived from PhxEco producer cells was harvested and T cells were virally transduced for 7 h at 37°C. T cells were allowed to recover and express the transgene for 60 h at 37°C, following intracellular flow cytometry to determine Foxp3 protein expression levels.

(B) Representative pseudocolor plots for ctrl MSCV virus and *Tcf7*-MSCV virus-treated T_{reg} cells. Virus-transduced cells are $CD90.1^+$, whereas non-transduced cells are $CD90.1^-$. From $CD90.1^+$ gate, Foxp3 expression can be determined. Numbers indicate positive cells in the gate in %. Axis labels indicate fluorescence intensity. MFI based on Foxp3 gate. Statistical quantification to the right (n = 7, unpaired t test, *$p < 0.05$ and ns $p > 0.05$).

(C) Experiment overview: Primary sorted *Foxp3*(GFP)-negative T_{conv} cells were FACS purified, stimulated with anti-CD3/28 beads, and differentiated with TGF-β for 48 h at 37°C. Then, virus-containing supernatant derived from PhxEco producer cells was harvested, and T cells were virally transduced for 7 h at 37°C. Afterward, T cells were allowed to recover and express the transgene for 60 h at 37°C, following intracellular flow cytometry to determine Foxp3 protein expression levels.

Figure 4. *Continued*

(D) Flow cytometry pseudocolor plots for T_{conv} cells treated with a control-MSCV virus or *Tcf7*-MSCV virus. From CD90.1$^+$ gate, Foxp3 expression can be determined. To the right, percentage of Foxp3 expression and Foxp3 MFI are evaluated across experiments (unpaired t test, n = 15, ***p < 0.001). Data are derived from two to three independent experiments with individual mice.

(wild-type) animals and detected no obvious differences (Figure 5A). In contrast to this, we observed about 5-fold elevated numbers of CD25-negative Foxp3-intermediate (CD4$^+$CD25$^-$Foxp3^{int}) T cells (1.56% in *Tcf7*$^{+/+}$ versus 8.82% in *Tcf7*$^{-/-}$). No dosage effect was observed, because heterozygous deletion of *Tcf7* had no effect. Next, we were interested in whether only CD4$^+$ T cells were affected by the deletion of TCF1. To answer this, we measured Foxp3 expression in CD8$^+$ T cells and CD19$^+$ B cells isolated from secondary lymphoid tissues of *Tcf7*$^{-/-}$, *Tcf7*$^{+/-}$, and *Tcf7*$^{+/+}$ animals (Figures 5B and 5C). In line with our observations with CD4$^+$ T cells, we could detect elevated numbers of Foxp3$^+$ cells in the CD8$^+$ population, although with a lower magnitude (Figure 5B). Interestingly, no effect was observed when analyzing Foxp3 expression in CD19$^+$ B cells (Figure 5C).

Are CD25$^-$Foxp3^{int} T cells actually T_{conv} cells that express Foxp3 due to the absence of TCF1, a Foxp3-repressive factor? To investigate this, we first measured Foxp3 protein levels via flow cytometry and detected reduced Foxp3 MFI of CD25$^-$Foxp3^{int} T_{reg} cells versus CD25$^+$Foxp3$^+$ "true" T_{reg} cells (Figure 5D). Next, we stained CTLA-4, a critical factor for T_{reg} identity and function (Figure 5E). Indeed, we also identified CTLA-4$^-$Foxp3$^+$ T cells, which are normally almost absent in wild-type animals (0.5% of CD4$^+$), but increased in TCF1-deficient animals to about 4% of CD4$^+$ T cells. The occurrence of this specific CD25$^-$CTLA4$^-$Foxp3^{int} population could be the consequence of a less restricted Foxp3 induction potential in TCF1-deficient T cells.

CRISPR-Cas9-Mediated Deletion of TCF1 Induces Foxp3 in Primary T_{conv} Cells

In *Tcf7*$^{-/-}$ animals, higher fractions of Foxp3-positive T cells were identified. However, these experiments did not tell us whether this was a consequence of an activation event in T_{conv} cells or a thymus-based selection process. To address the possibility that TCF1 restricts "unwanted" Foxp3 expression in T_{conv} cells, we deleted TCF1 in activated T_{conv} cells with CRISPR-Cas9 technology (Figure 6A). We calibrated the system by knocking out CD5 with a *Cd5* guide RNA (crRNA) and achieved a loss of CD5 protein expression in about 60% TCR-activated primary CD4$^+$ T cells (Figure 6B). Using *Tcf7* crRNA, we observed TCF1 protein loss in about 50% primary CD4$^+$ T cells (Figure 6B). Thus, individual wells contained equal ratios of TCF1-sufficient and TCF1-deficient CD4$^+$ T cells, allowing us to directly compare the effect of TCF1 loss on Foxp3 expression under the same conditions. Using different concentrations of TGF-β to induce Foxp3 expression, we identified significantly increased Foxp3 protein expression in TCF1-deleted T_{conv} cells when compared with TCF1-sufficient T_{conv} cells (Figure 6C).

To validate our findings in the human system, we used the CRISPR-Cas9 knockout approach to delete TCF1 in human CD4+ T cells. It has been described that a fraction of human CD4 T_{conv} cells spontaneously induces FOXP3 protein expression after TCR activation (Gavin et al., 2006; Walker et al., 2003). To test if TCF1 is relevant for this spontaneous FOXP3 expression, we stimulated human T_{conv} cells with anti-CD3 and anti-CD28 and observed the cells following CRISPR-Cas9 knockout of TCF1. Even without the addition of TGF-β, we detected significantly more FOXP3-expressing CD4$^+$ T cells in TCF1-deleted when compared with TCF1-sufficient T_{conv} cells (Figure 6D). The FOXP3-positive fraction increased from about 8% of CD4-sufficient T_{conv} cells to about 16% in TCF1-deleted T_{conv} cells. To investigate the inflammatory phenotype of TCF1-deleted FOXP3-positive T cells, we stimulated CRISPR-Cas9-treated T_{conv} cells with a T cell stimulation cocktail containing PMA/IM and blocked cytokine secretion with a transport inhibitor. Interestingly, TCF1-deleted FOXP3-positive T cells produced more interleukin-2 compared with control cells, indicating that TCF1-deleted FOXP3-positive T cells might indeed produce FOXP3 as a bystander effect of TCR stimulation, but do not exert the regulatory phenotype associated with a classical T_{reg} cell. Therefore, in summary, our data indicate that TCF1 protects T_{conv} cells from activation-induced FOXP3 expression.

DISCUSSION

Several TFs can bind to the *Foxp3* promoter. They modulate the downstream functions by direct binding to the promoter and initiation of transcription, via the recruitment of co-activators, by the selective displacement of repressive TFs, or by epigenetic modulation of the promoter (Delacher et al., 2014). It is believed that many factors co-operate in a context-dependent manner in a multiprotein network occupying the *Foxp3* promoter (Rudra et al., 2012).

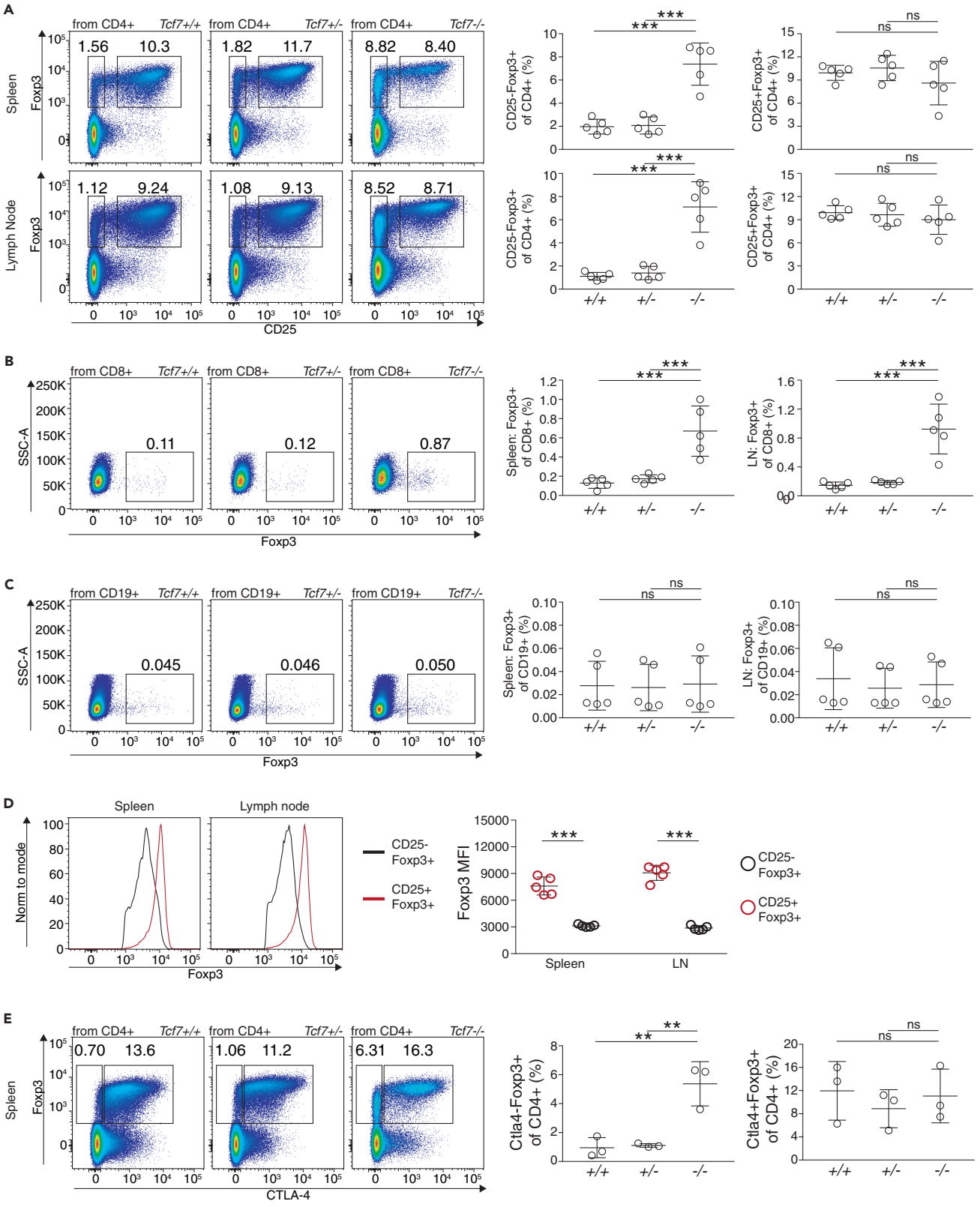
A
from CD4+ Tcf7+/+
from CD4+ Tcf7+/-
from CD4+ Tcf7-/-
Spleen
Lymph Node
Foxp3
CD25
1.56
10.3
1.82
11.7
8.82
8.40
1.12
9.24
1.08
9.13
8.52
8.71
CD25-Foxp3+ of CD4+ (%)
CD25+Foxp3+ of CD4+ (%)
***
ns
+/+
+/-
-/-
B
from CD8+ Tcf7+/+
from CD8+ Tcf7+/-
from CD8+ Tcf7-/-
SSC-A
Foxp3
0.11
0.12
0.87
Spleen: Foxp3+ of CD8+ (%)
LN: Foxp3+ of CD8+ (%)
C
from CD19+ Tcf7+/+
from CD19+ Tcf7+/-
from CD19+ Tcf7-/-
0.045
0.046
0.050
Spleen: Foxp3+ of CD19+ (%)
LN: Foxp3+ of CD19+ (%)
D
Spleen
Lymph node
Norm to mode
Foxp3
CD25- Foxp3+
CD25+ Foxp3+
Foxp3 MFI
LN
E
0.70
13.6
1.06
11.2
6.31
16.3
CTLA-4
Ctla4-Foxp3+ of CD4+ (%)
Ctla4+Foxp3+ of CD4+ (%)
**

Figure 5. CD25-Negative Foxp3-Intermediate T cells in TCF1-Deficient Mice

(A) Analysis of spleen and lymph node in *Tcf7*$^{-/-}$, *Tcf7*$^{-/+}$, and *Tcf7*$^{+/+}$ mice. CD4 T cells were identified (CD19^{-}CD8^{-}CD4^{+}), and Foxp3 versus CD25 was plotted. Percentage of CD25^{-}Foxp3^{+} and CD25^{+}Foxp3^{+} of CD4^{+} T cells was calculated (n = 5, one-way ANOVA with Tukey's post-test, ***p < 0.001).

(B) Analysis of spleen and lymph node in *Tcf7*$^{-/-}$, *Tcf7*$^{-/+}$, and *Tcf7*$^{+/+}$ mice. CD8 T cells were identified (CD19^{-}CD8^{+}CD4^{-}), and Foxp3 versus SSC-A was plotted. Percentage of Foxp3^{+} of CD8^{+} T cells was calculated (n = 5, one-way ANOVA with Tukey's post-test, ***p < 0.001).

(C) Analysis of spleen and lymph node in *Tcf7*$^{-/-}$, *Tcf7*$^{-/+}$, and *Tcf7*$^{+/+}$ mice. CD19 B cells were identified (CD19^{+}CD8^{-}CD4^{-}) and Foxp3 versus SSC-A was plotted. Percentage of Foxp3^{+} of CD19^{+} B cells was calculated (n = 5, one-way ANOVA with Tukey's post-test, ns p > 0.05).

(D) Expression of Foxp3 in CD25^{-}Foxp3^{+} and CD25^{+}Foxp3^{+} T cells from spleen and lymph node. Representative histograms to the left, and statistical quantification to the right (n = 5, one-way ANOVA with Sidak's post-test, ***p < 0.001).

(E) Percentage of CD25^{-}Ctla4^{+} and CD25^{+}Ctla4^{+} in spleens of *Tcf7*$^{-/-}$, *Tcf7*$^{-/+}$, and *Tcf7*$^{+/+}$ mice. Representative dot plots to the left, and statistical quantification to the right (n = 3, one-way ANOVA with Tukey's post-test, **p < 0.01 and ns p > 0.05). Data are derived from two or more independent experiments with individual mice.

In this study, we used an unbiased approach (Mittler et al., 2009) to determine binding partners to specific regions of the *Foxp3* gene promoter. As a source of protein, we used an EL4 T cell line. This cell line was shown to express *Foxp3* mRNA only upon TCR triggering with CD3-CD28 stimulation and TGF-β supplementation to the medium (Tone et al., 2008). Because we neither stimulated the TCR nor added TGF-β during expansion of EL4 cells, we probably identified a multiprotein complex protecting this T cell line from the "side effects" of *Foxp3* gene activity. Indeed, many of the candidate proteins were repressive factors actively down-regulating basic *Foxp3* promoter activity *in vitro*. This is in line with three other recent reports identifying cyclin-dependent kinases 8 and 19, the protein Yin-Yang 1, or the long noncoding RNA Flicr as repressors of Foxp3 protein expression (Akamatsu et al., 2019; Hwang et al., 2016; Zemmour et al., 2017).

Having established that our identified binding partners were *Foxp3* promoter suppressive in nature, we used a funnel approach to identify targets for further evaluation: we compared lists of factors that are down-regulated in Foxp3-expressing murine and human T_{reg} cells with our *Foxp3*-promoter-binding TFs. One interesting protein identified in the cross-comparison with both human and murine datasets was TCF1, a factor well known for its importance during thymic T cell development (Barra et al., 2015a, 2015b; Verbeek et al., 1995; Weber et al., 2011). It has also been described that TCF1 protein associates with Foxp3 and, via the Wnt signaling pathway, impairs suppressive function of T_{reg} cells (van Loosdregt et al., 2013). Testing TCF1 in a Luciferase screen, our data showed that TCF1 has *Foxp3*-promoter-suppressive capacity, and viral overexpression of TCF1 led to decreased Foxp3 expression *in vitro*. In a TCF1-deficient mouse strain, we detected an increase in a Foxp3-intermediate, but CD25-negative T cell population (CD25^{-}Foxp3^{int}). It is possible that, by deleting TCF1, we lowered the threshold for Foxp3 induction and thereby generated a population of CD25^{-}Foxp3^{int} T cells, otherwise almost absent in lymphoid tissues. As TCF1 has a strong influence on thymic differentiation of both T cells and T_{reg} cells (Barra et al., 2015a, 2015b; Verbeek et al., 1995; Weber et al., 2011), we wanted a more formal proof that TCF1 is involved in inhibiting FOXP3 expression in T_{conv} cells. Therefore, we deleted TCF1 using CRISPR-Cas9 knockout technology in primary mouse T_{conv} cells, which resulted in more Foxp3-expressing cells in the TCF1-deleted CD4^{+} T cell fraction.

Unlike in mice, in the human system, a certain percentage of T cells express FOXP3 upon activation *in vitro* (Gavin et al., 2006; Walker et al., 2003; Wang et al., 2007). To study whether activation-induced FOXP3 expression is TCF1 dependent, we used CRISPR-Cas9 technology to knockout TCF1 in human CD4 T_{conv} cells. We saw that spontaneous FOXP3 induction in activated human CD4^{+} T cells was significantly higher in TCF1-deficient T cells. This finding indicates an important function of TCF1 to suppress FOXP3 in activated non-T_{reg} CD4^{+} T cells. TCF1 expression also favors memory formation in T cells (Nish et al., 2017; Utzschneider et al., 2016; Zhou et al., 2010). Whether TCF1 expression protects memory T cells from unintentional expression of FOXP3 has to be further evaluated.

A recent study looked at the effects of TCF1 deletion on Foxp3 expression during thymic development. The authors could show that TCF1-deficient mice harbor an increased number of Foxp3-expressing double-negative cells in the thymus (Barra et al., 2015b). In line with our data, this publication reports that TCF1 is required to prevent premature expression of Foxp3 in the thymus. Another set of publications investigated the effect of a T_{reg}-specific knockout of TCF1 and Lef1 (Xing et al., 2019; Yang et al., 2019). Both studies showed that, whereas single-gene knockouts of Lef1 or TCF1 in T_{reg} cells had no catastrophic systemic effect, deleting both genes led to autoimmune disease by impairing the immunosuppressive function of T_{reg} cells. One of these studies closely examined the effect of a T_{reg} cell-specific TCF1 deletion on T_{reg} cell homeostasis and reported no perturbation (Xing et al., 2019). In contrast to this, we saw changes in the CD4 T cell compartment with TCF1 global knockout

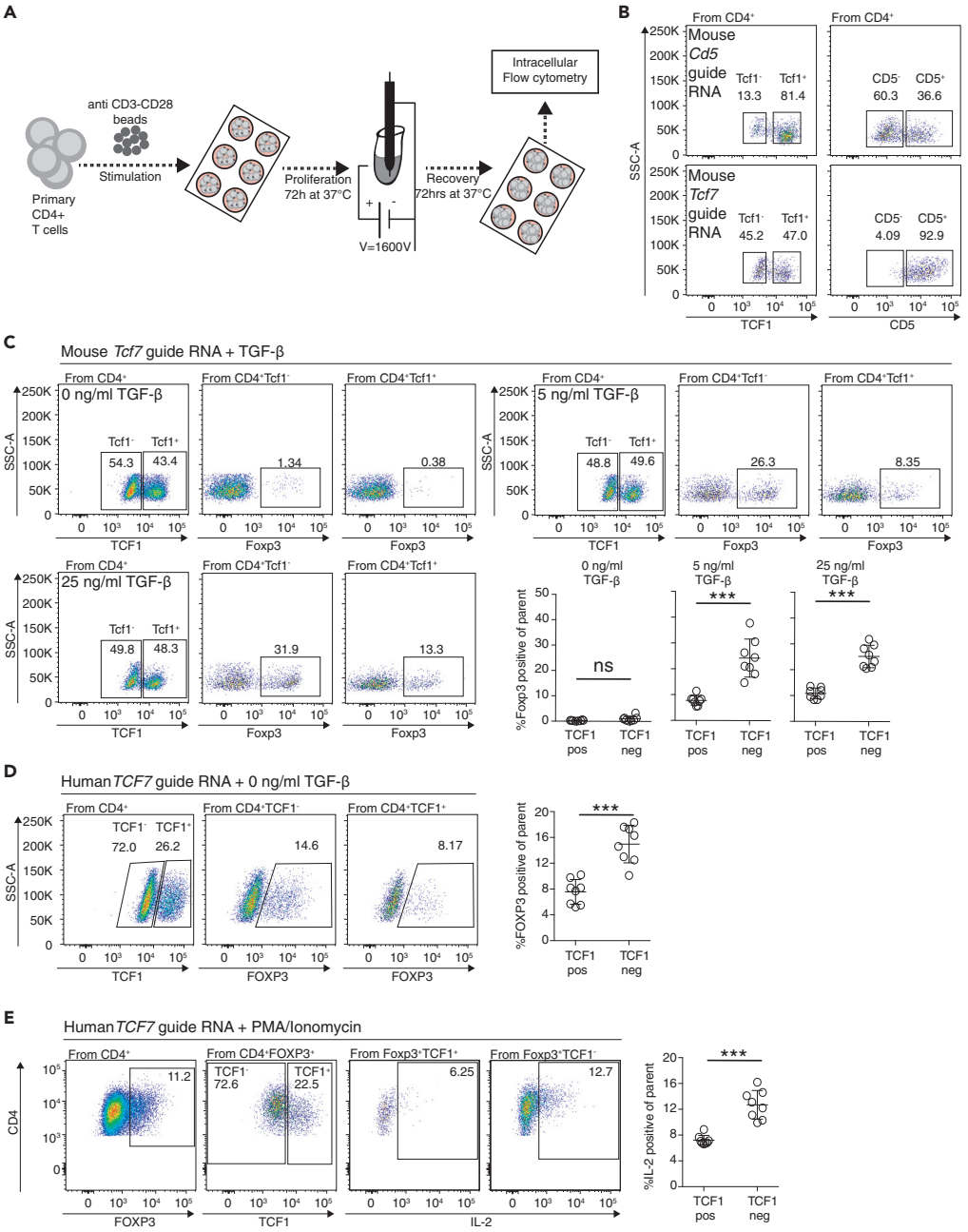

Figure 6. CRISPR-Cas9 Knockout of TCF1 Induces Elevated Foxp3 Levels

(A) Experiment overview: Primary murine CD4$^+$ T cells are stimulated with anti CD3-CD28 beads for 3 days *in vitro*. Then, cells are electroporated with a Cas9 protein, tracrRNA, and a *Tcf7* guide RNA with the Neon electroporation system. Afterward, cells recovered for 3 days at 37°C. Different concentrations of TGF-β were used during proliferation and recovery phase.

(B) CRISPR-Cas9-based deletion of CD5 (left) and TCF1 (right) in CD4+ T cells.

(C) Results of CRISPR-Cas9-based deletion of TCF1 in murine CD4$^+$ T cells. Pseudocolor dot plots illustrate TCF1-positive and TCF1-negative T cell populations after CRISPR-based TCF1 knockout and recovery for 72 h. Foxp3 expression for TCF1-negative and TCF1-positive populations shown to the right. A statistical verification across replicates is shown below (unpaired t test, n = 8, ***$p < 0.001$ and ns $p > 0.05$).

(D) Results of CRISPR-Cas9-based deletion of TCF1 in human CD4$^+$ T cells. Left, pseudocolor dot plots illustrating TCF1-positive and TCF1-negative T cell populations after CRISPR-based TCF1 knockout (*TCF7* AA guide RNA). Foxp3

Figure 6. *Continued*
expression for TCF1-negative and TCF1-positive populations is shown. A statistical verification across replicates is shown to the right (unpaired t test, n = 8, ***p < 0.001).
(E) Human FOXP3-negative T_{conv} cells were treated with *TCF7* AA guide RNA, followed by stimulation with PMA/Ionomycin and treatment with transport inhibitors. After 4 h, T cells were stained for intracellular expression of interleukin-2. A statistical verification across replicates is shown to the right (unpaired t test, n = 8, ***p > 0.001). Data are derived from two independent experiments with individual samples.

animals. Our animals, which also lack TCF1 in T_{conv} cells, showed the appearance of a Foxp3-intermediate, but CD25-negative T cell population ($CD25^{-}Foxp3^{int}$).

Whether our observation that TCF1 inhibits activation-induced FOXP3 expression in human and mouse conventional $CD4^{+}$ T cells is also transferable to other T cell subsets, specifically $CD8^{+}$ T cells, has to be further evaluated. Our mouse data showed an increased fraction of $CD8^{+}$ T cells expressing Foxp3 in TCF1-deficient versus TCF1-sufficient animals, although the overall magnitude was lower compared with the $CD4^{+}$ T cell compartment. Indeed, another study investigating $TCF1^{-/-}Lef1^{-/-}$ double knockout animals also reported an increased frequency of $CD8^{+}Foxp3^{+}$ T cells in the thymus (Xing et al., 2016). The authors reported intrinsic histone deacetylase activity of the TCF1 protein. Therefore, TCF1 could change the epigenetic accessibility of the *Foxp3* gene locus to prevent unwanted Foxp3 expression.

In summary, our study shows that TCF1 might be a key factor to protect T_{conv} cells from inadvertent Foxp3 expression. This allows unperturbed effector function of T cells while preventing the regulatory phenotype associated with Foxp3 expression.

Limitations of the Study

In this study, we present data about potential binding partners to the *Foxp3* promoter region, identified by mass spectrometry. Data were generated with a cell line (EL4), whereas follow-up experiments were conducted with primary human or murine T cells. In this article, we investigated TCF1 and the effects of overexpression or deletion on T cell biology, which could be extended by the analysis of other proteins identified with our screen.

Resource Availability

Lead Contact

Lead contact for this publication is Prof. Dr. Markus Feuerer.

Materials Availibility

Materials are available upon request by Prof. Dr. Markus Feuerer.

Data and Code Availability

Mass spectrometry data have been deposited to the ProteomeXchange Consortium under the PRIDE identifier PXD018764.

METHODS

All methods can be found in the accompanying Transparent Methods supplemental file.

SUPPLEMENTAL INFORMATION

Supplemental Information can be found online at https://doi.org/10.1016/j.isci.2020.101127.

ACKNOWLEDGMENTS

The *Foxp3* promoter Luciferase vector was a kind gift of Prof. Dr. Akihiko Yoshimura (Keio University, Japan). TCF1-deficient animals were a gift from Prof. Dr. Hans Clevers (Hubrecht Institute, Utrecht, The Netherlands). We thank the DKFZ core facilities Preclinical Research, Flow Cytometry, and Genomics & Proteomics, and the RCI flow cytometry core facility for technical support. We thank Sabine Schmitt (DKFZ), Marina Wuttke, Brigitte Ruhland, K.S., and Veronika Hofmann (all RCI) for technical support. We thank Dr. Simone Thomas for help with human samples. This work was supported by grants from the European Research Council (ERC-CoG, #648145 REGiREG) to M.F., and by the Deutsche Forschungsgemeinschaft

(DFG, German Research Foundation)—Projektnummer 324392634—TRR 221 to M.F., M.D. was supported by the German-Israeli Helmholtz Research School in Cancer Biology.

AUTHOR CONTRIBUTIONS

M.D., M.M.B., J.K., J.A., and M.F. designed experiments; M.D., M.M.B., Y.H., K.E., M.-R.R., D.M.R., U.T., A.-C.H., A.K., K.L.B., M.G.., L.W., and K.S. performed the experiments; M.D., K.E., C.D.I., J.A., J.K., and M.F. analyzed data; M.D. and M.F. wrote the manuscript.

DECLARATION OF INTERESTS

The authors declare no competing financial interests.

Received: March 3, 2020
Revised: April 2, 2020
Accepted: April 29, 2020
Published: May 22, 2020

REFERENCES

Akamatsu, M., Mikami, N., Ohkura, N., Kawakami, R., Kitagawa, Y., Sugimoto, A., Hirota, K., Nakamura, N., Ujihara, S., Kurosaki, T., et al. (2019). Conversion of antigen-specific effector/memory T cells into Foxp3-expressing Treg cells by inhibition of CDK8/19. Sci. Immunol. *4*, eaaw2707.

Andersen, K.G., Nissen, J.K., and Betz, A.G. (2012). Comparative genomics reveals key gain-of-function events in Foxp3 during regulatory T cell evolution. Front. Immunol. *3*, 113.

Barra, M.M., Richards, D.M., Hansson, J., Hofer, A.C., Delacher, M., Hettinger, J., Krijgsveld, J., and Feuerer, M. (2015a). Transcription factor 7 limits regulatory T cell generation in the thymus. J. Immunol. *195*, 3058–3070.

Barra, M.M., Richards, D.M., Hofer, A.C., Delacher, M., and Feuerer, M. (2015b). Premature expression of Foxp3 in double-negative thymocytes. PLoS One *10*, e0127038.

Bennett, C.L., Christie, J., Ramsdell, F., Brunkow, M.E., Ferguson, P.J., Whitesell, L., Kelly, T.E., Saulsbury, F.T., Chance, P.F., and Ochs, H.D. (2001). The immune dysregulation, polyendocrinopathy, enteropathy, X-linked syndrome (IPEX) is caused by mutations of FOXP3. Nat. Genet. *27*, 20–21.

Brunkow, M.E., Jeffery, E.W., Hjerrild, K.A., Paeper, B., Clark, L.B., Yasayko, S.A., Wilkinson, J.E., Galas, D., Ziegler, S.F., and Ramsdell, F. (2001). Disruption of a new forkhead/winged-helix protein, scurfin, results in the fatal lymphoproliferative disorder of the scurfy mouse. Nat. Genet. *27*, 68–73.

Bruno, L., Mazzarella, L., Hoogenkamp, M., Hertweck, A., Cobb, B.S., Sauer, S., Hadjur, S., Leleu, M., Naoe, Y., Telfer, J.C., et al. (2009). Runx proteins regulate Foxp3 expression. J. Exp. Med. *206*, 2329–2337.

Burchill, M.A., Yang, J., Vogtenhuber, C., Blazar, B.R., and Farrar, M.A. (2007). IL-2 receptor beta-dependent STAT5 activation is required for the development of Foxp3+ regulatory T cells. J. Immunol. *178*, 280–290.

Cuadrado, E., van den Biggelaar, M., de Kivit, S., Chen, Y.Y., Slot, M., Doubal, I., Meijer, A., van Lier, R.A.W., Borst, J., and Amsen, D. (2018). Proteomic analyses of human regulatory T cells reveal adaptations in signaling pathways that protect cellular identity. Immunity *48*, 1046–1059.e6.

Delacher, M., Imbusch, C.D., Hotz-Wagenblatt, A., Mallm, J.P., Bauer, K., Simon, M., Riegel, D., Rendeiro, A.F., Bittner, S., Sanderink, L., et al. (2020). Precursors for nonlymphoid-tissue Treg cells reside in secondary lymphoid organs and are programmed by the transcription factor BATF. Immunity *52*, 295–312.e11.

Delacher, M., Imbusch, C.D., Weichenhan, D., Breiling, A., Hotz-Wagenblatt, A., Trager, U., Hofer, A.C., Kagebein, D., Wang, Q., Frauhammer, F., et al. (2017). Genome-wide DNA-methylation landscape defines specialization of regulatory T cells in tissues. Nat. Immunol. *18*, 1160–1172.

Delacher, M., Schmidl, C., Herzig, Y., Breloer, M., Hartmann, W., Brunk, F., Kagebein, D., Trager, U., Hofer, A.C., Bittner, S., et al. (2019). Rbpj expression in regulatory T cells is critical for restraining TH2 responses. Nat. Commun. *10*, 1621.

Delacher, M., Schreiber, L., Richards, D.M., Farah, C., Feuerer, M., and Huehn, J. (2014). Transcriptional control of regulatory T cells. Curr. Top. Microbiol. Immunol. *381*, 83–124.

Floess, S., Freyer, J., Siewert, C., Baron, U., Olek, S., Polansky, J., Schlawe, K., Chang, H.D., Bopp, T., Schmitt, E., et al. (2007). Epigenetic control of the foxp3 locus in regulatory T cells. PLoS Biol. *5*, e38.

Fontenot, J.D., Gavin, M.A., and Rudensky, A.Y. (2003). Foxp3 programs the development and function of CD4+CD25+ regulatory T cells. Nat. Immunol. *4*, 330–336.

Gavin, M.A., Torgerson, T.R., Houston, E., DeRoos, P., Ho, W.Y., Stray-Pedersen, A., Ocheltree, E.L., Greenberg, P.D., Ochs, H.D., and Rudensky, A.Y. (2006). Single-cell analysis of normal and FOXP3-mutant human T cells: FOXP3 expression without regulatory T cell development. Proc. Natl. Acad. Sci. U S A *103*, 6659–6664.

Harada, Y., Harada, Y., Elly, C., Ying, G., Paik, J.H., DePinho, R.A., and Liu, Y.C. (2010). Transcription factors Foxo3a and Foxo1 couple the E3 ligase Cbl-b to the induction of Foxp3 expression in induced regulatory T cells. J. Exp. Med. *207*, 1381–1391.

Hwang, S.S., Jang, S.W., Kim, M.K., Kim, L.K., Kim, B.S., Kim, H.S., Kim, K., Lee, W., Flavell, R.A., and Lee, G.R. (2016). YY1 inhibits differentiation and function of regulatory T cells by blocking Foxp3 expression and activity. Nat. Commun. *7*, 10789.

Janson, P.C., Winerdal, M.E., Marits, P., Thorn, M., Ohlsson, R., and Winqvist, O. (2008). FOXP3 promoter demethylation reveals the committed Treg population in humans. PLoS One *3*, e1612.

Josefowicz, S.Z., Niec, R.E., Kim, H.Y., Treuting, P., Chinen, T., Zheng, Y., Umetsu, D.T., and Rudensky, A.Y. (2012). Extrathymically generated regulatory T cells control mucosal TH2 inflammation. Nature *482*, 395–399.

Kim, H.P., and Leonard, W.J. (2007). CREB/ATF-dependent T cell receptor-induced FoxP3 gene expression: a role for DNA methylation. J. Exp. Med. *204*, 1543–1551.

Kitagawa, Y., Ohkura, N., Kidani, Y., Vandenbon, A., Hirota, K., Kawakami, R., Yasuda, K., Motooka, D., Nakamura, S., Kondo, M., et al. (2017). Guidance of regulatory T cell development by Satb1-dependent super-enhancer establishment. Nat. Immunol. *18*, 173–183.

Klunker, S., Chong, M.M., Mantel, P.Y., Palomares, O., Bassin, C., Ziegler, M., Ruckert, B., Meiler, F., Akdis, M., Littman, D.R., and Akdis, C.A. (2009). Transcription factors RUNX1 and RUNX3 in the induction and suppressive function of Foxp3+ inducible regulatory T cells. J. Exp. Med. *206*, 2701–2715.

Mantel, P.Y., Ouaked, N., Ruckert, B., Karagiannidis, C., Welz, R., Blaser, K., and Schmidt-Weber, C.B. (2006). Molecular mechanisms underlying FOXP3 induction in human T cells. J. Immunol. *176*, 3593–3602.

Mayor, C., Brudno, M., Schwartz, J.R., Poliakov, A., Rubin, E.M., Frazer, K.A., Pachter, L.S., and Dubchak, I. (2000). Vista : visualizing global DNA sequence alignments of arbitrary length. Bioinformatics *16*, 1046–1047.

Mittler, G., Butter, F., and Mann, M. (2009). A SILAC-based DNA protein interaction screen that identifies candidate binding proteins to functional DNA elements. Genome Res. *19*, 284–293.

Mouly, E., Chemin, K., Nguyen, H.V., Chopin, M., Mesnard, L., Leite-de-Moraes, M., Burlen-defranoux, O., Bandeira, A., and Bories, J.C. (2010). The Ets-1 transcription factor controls the development and function of natural regulatory T cells. J. Exp. Med. *207*, 2113–2125.

Nish, S.A., Zens, K.D., Kratchmarov, R., Lin, W.W., Adams, W.C., Chen, Y.H., Yen, B., Rothman, N.J., Bhandoola, A., Xue, H.H., et al. (2017). CD4+ T cell effector commitment coupled to self-renewal by asymmetric cell divisions. J. Exp. Med. *214*, 39–47.

Oh-Hora, M., Komatsu, N., Pishyareh, M., Feske, S., Hori, S., Taniguchi, M., Rao, A., and Takayanagi, H. (2013). Agonist-selected T cell development requires strong T cell receptor signaling and store-operated calcium entry. Immunity *38*, 881–895.

Ohkura, N., Hamaguchi, M., Morikawa, H., Sugimura, K., Tanaka, A., Ito, Y., Osaki, M., Tanaka, Y., Yamashita, R., Nakano, N., et al. (2012). T cell receptor stimulation-induced epigenetic changes and Foxp3 expression are independent and complementary events required for Treg cell development. Immunity *37*, 785–799.

Ouyang, W., Beckett, O., Ma, Q., Paik, J.H., DePinho, R.A., and Li, M.O. (2010). Foxo proteins cooperatively control the differentiation of Foxp3+ regulatory T cells. Nat. Immunol. *11*, 618–627.

Ruan, Q., Kameswaran, V., Tone, Y., Li, L., Liou, H.C., Greene, M.I., Tone, M., and Chen, Y.H. (2009). Development of Foxp3(+) regulatory t cells is driven by the c-Rel enhanceosome. Immunity *31*, 932–940.

Rudensky, A.Y. (2011). Regulatory T cells and Foxp3. Immunol. Rev. *241*, 260–268.

Rudra, D., deRoos, P., Chaudhry, A., Niec, R.E., Arvey, A., Samstein, R.M., Leslie, C., Shaffer, S.A., Goodlett, D.R., and Rudensky, A.Y. (2012). Transcription factor Foxp3 and its protein partners form a complex regulatory network. Nat. Immunol. *13*, 1010–1019.

Sadlon, T.J., Wilkinson, B.G., Pederson, S., Brown, C.Y., Bresatz, S., Gargett, T., Melville, E.L., Peng, K., D'Andrea, R.J., Glonek, G.G., et al. (2010). Genome-wide identification of human FOXP3 target genes in natural regulatory T cells. J. Immunol. *185*, 1071–1081.

Schlenner, S.M., Weigmann, B., Ruan, Q., Chen, Y., and von Boehmer, H. (2012). Smad3 binding to the foxp3 enhancer is dispensable for the development of regulatory T cells with the exception of the gut. J. Exp. Med. *209*, 1529–1535.

Schmidl, C., Delacher, M., Huehn, J., and Feuerer, M. (2018). Epigenetic mechanisms regulating T-cell responses. J. Allergy Clin. Immunol. *142*, 728–743.

Schuster, M., Glauben, R., Plaza-Sirvent, C., Schreiber, L., Annemann, M., Floess, S., Kuhl, A.A., Clayton, L.K., Sparwasser, T., Schulze-Osthoff, K., et al. (2012). IkappaB(NS) protein mediates regulatory T cell development via induction of the Foxp3 transcription factor. Immunity *37*, 998–1008.

Sekiya, T., Kashiwagi, I., Inoue, N., Morita, R., Hori, S., Waldmann, H., Rudensky, A.Y., Ichinose, H., Metzger, D., Chambon, P., and Yoshimura, A. (2011). The nuclear orphan receptor Nr4a2 induces Foxp3 and regulates differentiation of CD4+ T cells. Nat. Commun. *2*, 269.

Sekiya, T., Kashiwagi, I., Yoshida, R., Fukaya, T., Morita, R., Kimura, A., Ichinose, H., Metzger, D., Chambon, P., and Yoshimura, A. (2013). Nr4a receptors are essential for thymic regulatory T cell development and immune homeostasis. Nat. Immunol. *14*, 230–237.

Tone, Y., Furuuchi, K., Kojima, Y., Tykocinski, M.L., Greene, M.I., and Tone, M. (2008). Smad3 and NFAT cooperate to induce Foxp3 expression through its enhancer. Nat. Immunol. *9*, 194–202.

Utzschneider, D.T., Charmoy, M., Chennupati, V., Pousse, L., Ferreira, D.P., Calderon-Copete, S., Danilo, M., Alfei, F., Hofmann, M., Wieland, D., et al. (2016). T cell factor 1-expressing memory-like CD8(+) T cells sustain the immune response to chronic viral infections. Immunity *45*, 415–427.

van Loosdregt, J., Fleskens, V., Tiemessen, M.M., Mokry, M., van Boxtel, R., Meerding, J., Pals, C.E., Kurek, D., Baert, M.R., Delemarre, E.M., et al. (2013). Canonical Wnt signaling negatively modulates regulatory T cell function. Immunity *39*, 298–310.

Verbeek, S., Izon, D., Hofhuis, F., Robanus-Maandag, E., te Riele, H., van de Wetering, M., Oosterwegel, M., Wilson, A., MacDonald, H.R., and Clevers, H. (1995). An HMG-box-containing T-cell factor required for thymocyte differentiation. Nature *374*, 70–74.

Walker, M.R., Kasprowicz, D.J., Gersuk, V.H., Benard, A., Van Landeghen, M., Buckner, J.H., and Ziegler, S.F. (2003). Induction of FoxP3 and acquisition of T regulatory activity by stimulated human CD4+CD25- T cells. J. Clin. Invest. *112*, 1437–1443.

Wang, J., Ioan-Facsinay, A., van der Voort, E.I., Huizinga, T.W., and Toes, R.E. (2007). Transient expression of FOXP3 in human activated nonregulatory CD4+ T cells. Eur. J. Immunol. *37*, 129–138.

Wang, Y., Su, M.A., and Wan, Y.Y. (2011). An essential role of the transcription factor GATA-3 for the function of regulatory T cells. Immunity *35*, 337–348.

Weber, B.N., Chi, A.W., Chavez, A., Yashiro-Ohtani, Y., Yang, Q., Shestova, O., and Bhandoola, A. (2011). A critical role for TCF-1 in T-lineage specification and differentiation. Nature *476*, 63–68.

Wildin, R.S., Ramsdell, F., Peake, J., Faravelli, F., Casanova, J.L., Buist, N., Levy-Lahad, E., Mazzella, M., Goulet, O., Perroni, L., et al. (2001). X-linked neonatal diabetes mellitus, enteropathy and endocrinopathy syndrome is the human equivalent of mouse scurfy. Nat. Genet. *27*, 18–20.

Wohlfert, E.A., Grainger, J.R., Bouladoux, N., Konkel, J.E., Oldenhove, G., Ribeiro, C.H., Hall, J.A., Yagi, R., Naik, S., Bhairavabhotla, R., et al. (2011). GATA3 controls Foxp3(+) regulatory T cell fate during inflammation in mice. J. Clin. Invest. *121*, 4503–4515.

Xie, X., Stubbington, M.J., Nissen, J.K., Andersen, K.G., Hebenstreit, D., Teichmann, S.A., and Betz, A.G. (2015). The regulatory T cell lineage factor Foxp3 regulates gene expression through several distinct mechanisms mostly independent of direct DNA binding. PLoS Genet. *11*, e1005251.

Xing, S., Gai, K., Li, X., Shao, P., Zeng, Z., Zhao, X., Zhao, X., Chen, X., Paradee, W.J., Meyerholz, D.K., et al. (2019). Tcf1 and Lef1 are required for the immunosuppressive function of regulatory T cells. J. Exp. Med. *216*, 847–866.

Xing, S., Li, F., Zeng, Z., Zhao, Y., Yu, S., Shan, Q., Li, Y., Phillips, F.C., Maina, P.K., Qi, H.H., et al. (2016). Tcf1 and Lef1 transcription factors establish CD8(+) T cell identity through intrinsic HDAC activity. Nat. Immunol. *17*, 695–703.

Yang, B.H., Wang, K., Wan, S., Liang, Y., Yuan, X., Dong, Y., Cho, S., Xu, W., Jepsen, K., Feng, G.S., et al. (2019). TCF1 and LEF1 control Treg competitive survival and Tfr development to prevent autoimmune diseases. Cell Rep. *27*, 3629–3645.e6.

Yao, Z., Kanno, Y., Kerenyi, M., Stephens, G., Durant, L., Watford, W.T., Laurence, A., Robinson, G.W., Shevach, E.M., Moriggl, R., et al. (2007). Nonredundant roles for Stat5a/b in directly regulating Foxp3. Blood *109*, 4368–4375.

Zemmour, D., Pratama, A., Loughhead, S.M., Mathis, D., and Benoist, C. (2017). Flicr, a long noncoding RNA, modulates Foxp3 expression and autoimmunity. Proc. Natl. Acad. Sci. U S A *114*, E3472–E3480.

Zheng, Y., Josefowicz, S., Chaudhry, A., Peng, X.P., Forbush, K., and Rudensky, A.Y. (2010). Role of conserved non-coding DNA elements in the Foxp3 gene in regulatory T-cell fate. Nature *463*, 808–812.

Zhou, X., Yu, S., Zhao, D.M., Harty, J.T., Badovinac, V.P., and Xue, H.H. (2010). Differentiation and persistence of memory CD8(+) T cells depend on T cell factor 1. Immunity *33*, 229–240.

iScience, Volume *23*

Supplemental Information

Quantitative Proteomics Identifies TCF1 as a Negative Regulator of *Foxp3* Expression in Conventional T Cells

Michael Delacher, Melanie M. Barra, Yonatan Herzig, Katrin Eichelbaum, Mahmoud-Reza Rafiee, David M. Richards, Ulrike Träger, Ann-Cathrin Hofer, Alexander Kazakov, Kathrin L. Braband, Marina Gonzalez, Lukas Wöhrl, Kathrin Schambeck, Charles D. Imbusch, Jakub Abramson, Jeroen Krijgsveld, and Markus Feuerer

Figure S1

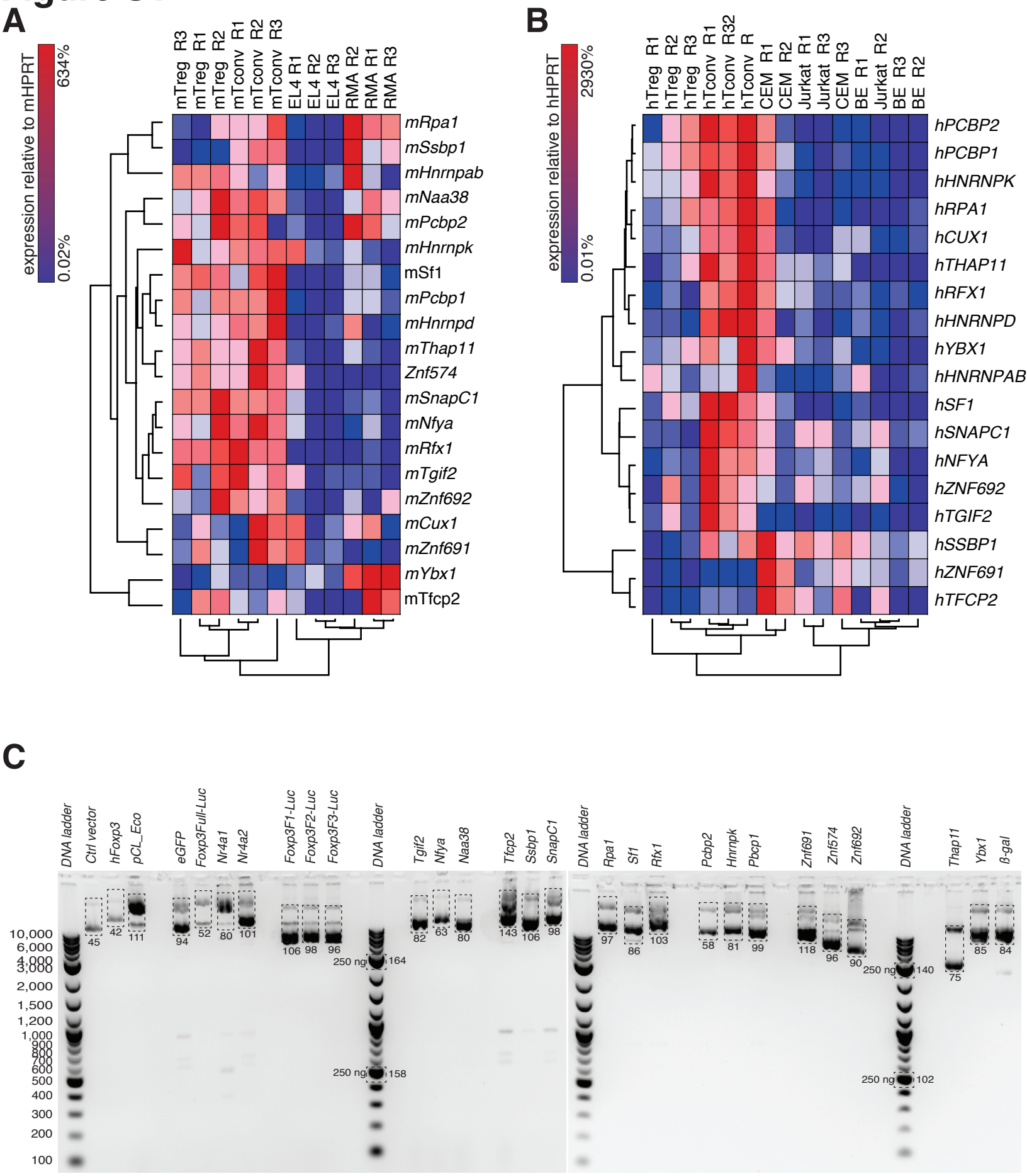
A
expression relative to mHPRT
634%
0.02%
mTreg R3
mTreg R1
mTreg R2
mTconv R1
mTconv R2
mTconv R3
EL4 R1
EL4 R2
EL4 R3
RMA R2
RMA R1
RMA R3
mRpa1
mSsbp1
mHnrnpab
mNaa38
mPcbp2
mHnrnpk
mSf1
mPcbp1
mHnrnpd
mThap11
Znf574
mSnapC1
mNfya
mRfx1
mTgif2
mZnf692
mCux1
mZnf691
mYbx1
mTfcp2
B
expression relative to hHPRT
2930%
0.01%
hTreg R1
hTreg R2
hTreg R3
hTconv R1
hTconv R32
hTconv R
CEM R1
CEM R2
Jurkat R1
Jurkat R3
CEM R3
BE R1
Jurkat R2
BE R3
BE R2
hPCBP2
hPCBP1
hHNRNPK
hRPA1
hCUX1
hTHAP11
hRFX1
hHNRNPD
hYBX1
hHNRNPAB
hSF1
hSNAPC1
hNFYA
hZNF692
hTGIF2
hSSBP1
hZNF691
hTFCP2

C

DNA ladder
Ctrl vector
hFoxp3
pCL_Eco
eGFP
Foxp3Full-Luc
Nr4a1
Nr4a2
Foxp3F1-Luc
Foxp3F2-Luc
Foxp3F3-Luc
DNA ladder
Tgif2
Nfya
Naa38
Tfcp2
Ssbp1
SnapC1
DNA ladder
Rpa1
Sf1
Rfx1
Pcbp2
Hnrnpk
Pbcp1
Znf691
Znf574
Znf692
DNA ladder
Thap11
Ybx1
β-gal
10,000
6,000
4,000
3,000
2,000
1,500
1,200
1,000
900
800
700
600
500
400
300
200
100
45
42
111
94
52
80
101
106
98
96
250 ng
164
250 ng
158
82
63
80
143
106
98
97
86
103
58
81
99
118
96
90
250 ng
140
250 ng
102
75
85
84

Figure S1. Gene expression and plasmid stability, related to Figure 2. (**A**) Gene expression of candidate transcription factors in primary murine T_{reg} or T_{conv} cells or cell lines. Rows: different genes; Columns: different replicates of samples; heatmap row-normalized, n=3. (**B**) Gene expression of candidate transcription factors in primary human T_{reg} or T_{conv} cells or cell lines. Rows: different genes; Columns: different replicates of samples; heatmap row-normalized, n=3. (**C**) Plasmid stability and size analysis: different vectors (Luciferase vectors, eukaryotic production vectors, viral production vectors) were linearized and separated on agarose gel to visualize plasmid integrity. Numbers indicate concentration by measuring dark values in rectangular section.

Figure S2

A

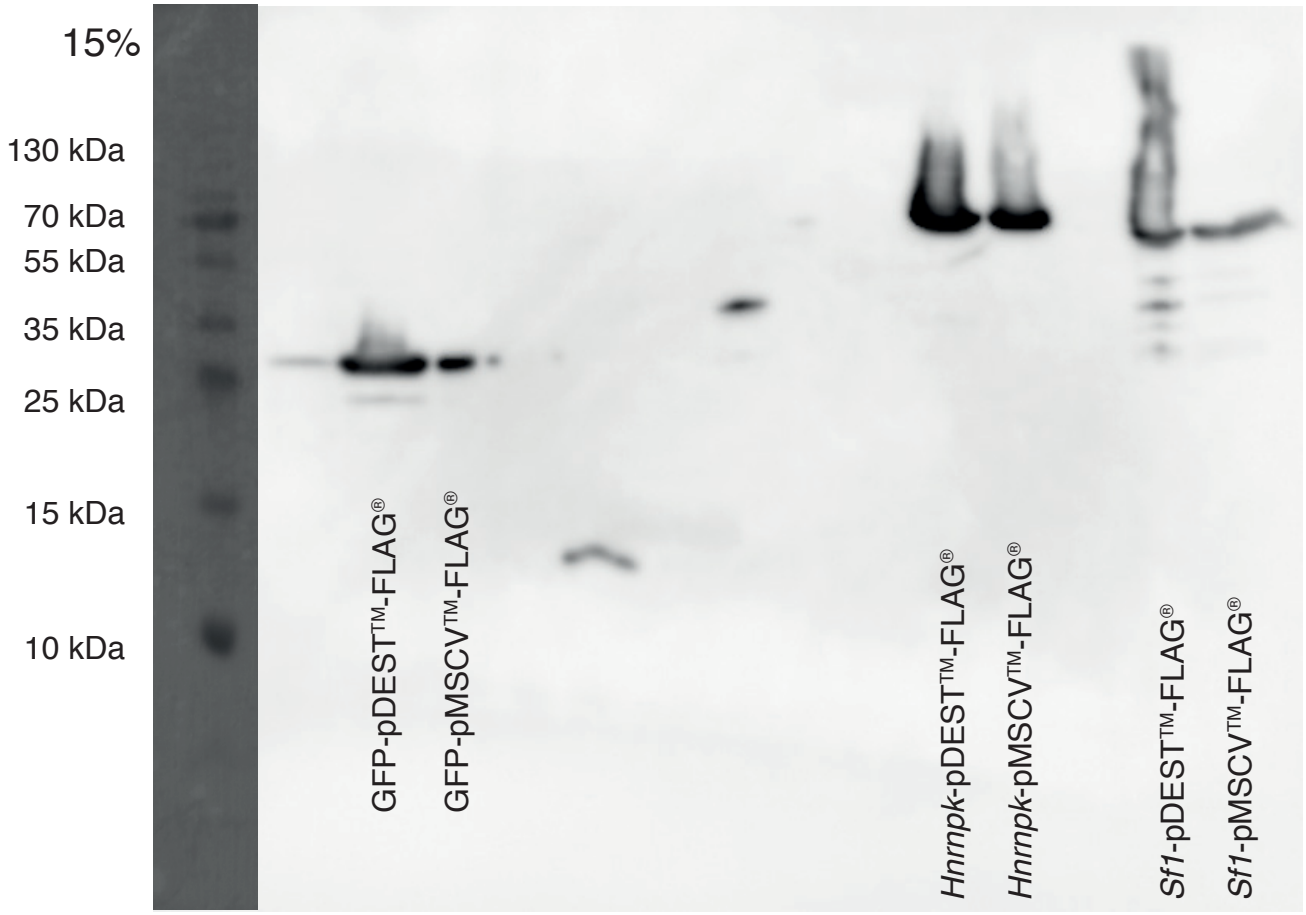

B

Gene expression (%Gapdh)

	Transfected pDEST plasmid																	
Plasmid		*Hnrnpk*	*Rpa1*	*Naa38*	*Tgif2*	*Znf574*	*Thap11*	*Ybx1*	*Pcbp2*	*Pcbp1*	*Ssbp1*	*Nfya*	*Snapc1*	*Znf691*	*Rfx1*	*Sf1*	*Znf692*	*Tfcp2*
Plasmid ID	H2O	252	248	244	242	255	257	258	251	253	246	243	247	254	250	249	256	245
mHnrnpk	0,00	**85,40**	0,20	0,20	0,20	0,30	0,20	0,40	1,20	0,90	0,00	0,00	0,00	0,40	0,30	1,00	1,40	2,80
mRpa1	0,00	0,00	**174,50**	0,00	0,00	0,00	0,00	0,00	0,00	0,00	0,00	0,00	0,00	0,00	0,00	0,00	0,00	0,00
mNaa38	0,00	0,00	0,00	**1043,20**	0,00	0,00	0,00	0,00	0,00	0,00	0,00	0,00	0,00	0,00	0,00	0,00	0,00	0,00
mTgif2	0,00	0,00	0,00	0,00	**177,20**	0,00	0,00	0,00	0,00	0,00	0,01	0,08	0,00	0,01	0,01	0,02	0,05	0,08
mZnf574	0,00	0,00	0,00	0,00	0,00	**8,60**	0,00	0,00	0,00	0,00	0,00	0,00	0,00	0,00	0,00	0,00	0,00	0,00
mThap11	0,00	0,10	0,10	0,10	0,00	0,10	**97,70**	0,10	0,00	0,10	0,11	0,09	0,00	0,10	0,06	0,07	0,06	0,07
mYbx1	0,00	18,20	22,60	24,90	29,10	21,50	32,40	**478,30**	45,50	46,80	35,65	44,75	34,92	42,43	23,83	44,78	33,17	40,05
mPcbp2	0,00	6,20	5,80	7,20	6,70	5,10	6,00	9,30	**208,60**	7,40	8,62	7,41	7,39	8,26	4,26	8,15	4,91	5,39
mPcbp1	0,00	0,00	0,00	0,00	0,00	0,00	0,00	0,00	0,00	**1008,40**	0,01	0,01	0,01	0,01	0,00	0,01	0,01	0,02
mSsbp1	0,00	0,00	0,00	0,00	0,00	0,00	0,00	0,10	0,10	0,10	**28,50**	0,01	0,01	0,01	0,01	0,01	0,01	0,02
mNfya	0,00	0,00	0,00	0,00	0,00	0,00	0,00	0,10	0,10	0,10	0,04	**201,67**	0,04	0,07	0,03	0,06	0,04	0,05
mSnapc1	0,00	0,00	0,00	0,00	0,00	0,00	0,00	0,00	0,00	0,00	0,00	0,00	**281,28**	0,00	0,00	0,00	0,00	0,00
mZnf691	0,00	0,00	0,00	0,00	0,00	0,10	0,00	0,00	0,00	0,00	0,00	0,00	0,00	**672,72**	0,00	0,00	0,00	0,00
mRfx1	0,00	0,00	0,00	0,00	0,00	0,00	0,00	0,00	0,00	0,00	**42,69**	0,00	0,00	0,00	**0,64**	0,00	0,00	0,00
mSf1	0,00	0,00	0,00	0,00	0,00	0,00	0,00	0,00	0,00	0,00	0,01	0,01	0,03	0,01	0,00	**153,58**	0,01	0,00
mZnf692	0,00	0,00	0,00	0,00	0,00	0,00	0,00	0,00	0,00	0,00	0,00	0,00	0,00	0,00	0,00	0,00	**42,37**	0,00
mTfcp2	0,00	0,00	0,00	0,00	0,00	0,00	0,00	0,00	0,00	0,00	0,00	0,00	0,00	0,00	0,00	0,00	0,00	**356,77**

Top 1 or top 2 item (s) highlighted in red and bold

Figure S2. Transgene expression and plasmid identity, related to Figure 2. (**A**) Western Blot with lysates of producer cell lines transfected with either pDEST eukaryotic production vectors or pMSCV viral production vectors. Recombinant proteins were FLAG-labeled and detected with anti-FLAG antibodies. Protein ladder to the left. (**B**) Eukaryotic production vectors were transfected into production cell lines. Afterwards, cells were lysed and RNA was isolated. cDNA was generated and gene expression was measured by qPCR. Rows = different qPCR primers; Columns: different eukaryotic production vectors used to transfect target cells.

Figure S3

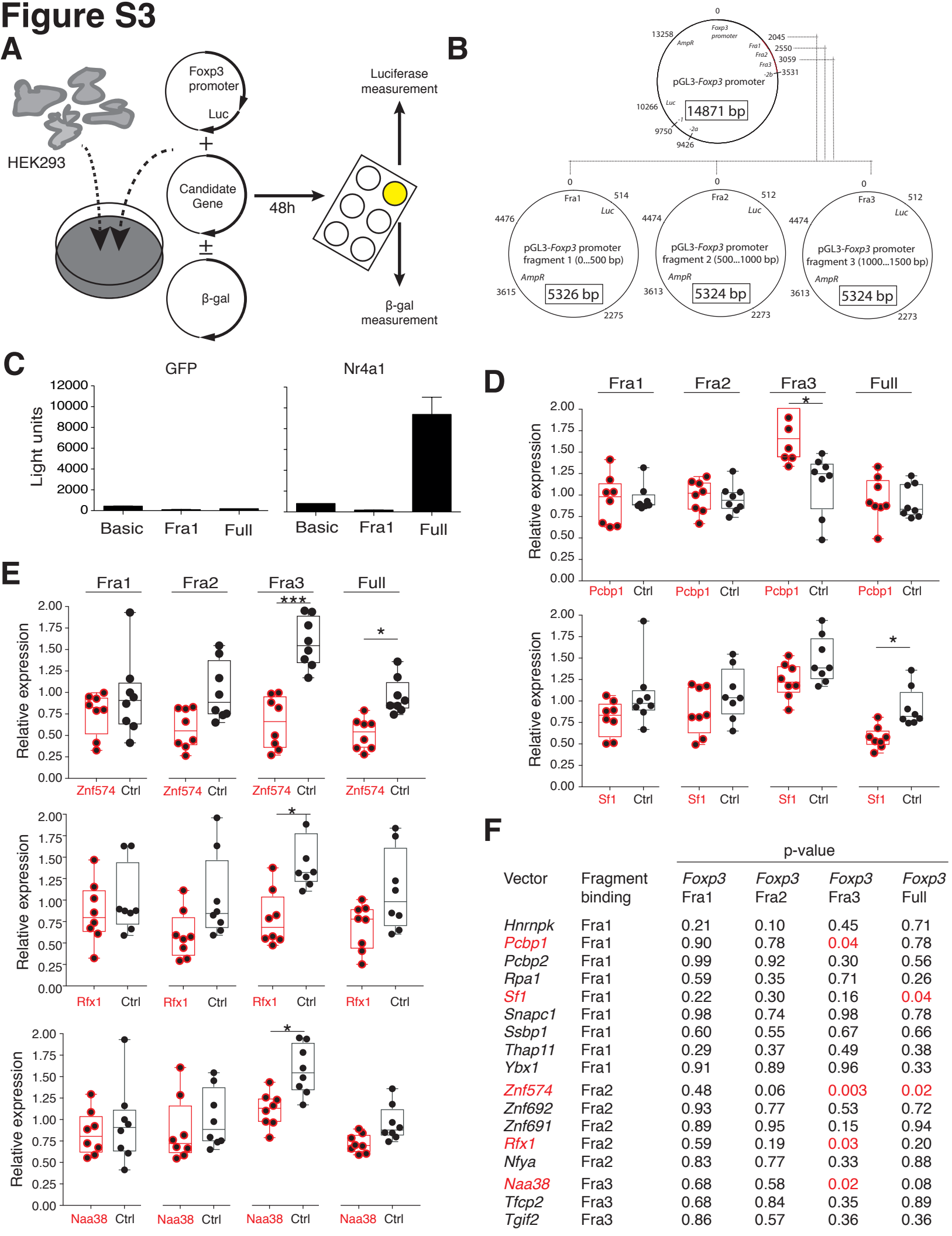

Vector	Fragment binding	p-value *Foxp3* Fra1	*Foxp3* Fra2	*Foxp3* Fra3	*Foxp3* Full
Hnrnpk	Fra1	0.21	0.10	0.45	0.71
Pcbp1	Fra1	0.90	0.78	0.04	0.78
Pcbp2	Fra1	0.99	0.92	0.30	0.56
Rpa1	Fra1	0.59	0.35	0.71	0.26
Sf1	Fra1	0.22	0.30	0.16	0.04
Snapc1	Fra1	0.98	0.74	0.98	0.78
Ssbp1	Fra1	0.60	0.55	0.67	0.66
Thap11	Fra1	0.29	0.37	0.49	0.38
Ybx1	Fra1	0.91	0.89	0.96	0.33
Znf574	Fra2	0.48	0.06	0.003	0.02
Znf692	Fra2	0.93	0.77	0.53	0.72
Znf691	Fra2	0.89	0.95	0.15	0.94
Rfx1	Fra2	0.59	0.19	0.03	0.20
Nfya	Fra2	0.83	0.77	0.33	0.88
Naa38	Fra3	0.68	0.58	0.02	0.08
Tfcp2	Fra3	0.68	0.84	0.35	0.89
Tgif2	Fra3	0.86	0.57	0.36	0.36

Figure S3. Testing of candidate factors with *Foxp3*-Luciferase vectors in HEK293 cells, related to Figure 2. (**A**) Experiment overview: 50,000 HEK293 cells were seeded in a 96-well flat-bottom plate and transfected with 3 vectors 24h later: β-galactosidase normalization vector, *Foxp3*-Luciferase reporter vector, and a eukaryotic expression vector containing the transgene of interest. After 48 h, cells were lysed and β-galactosidase as well as luciferase enzymatic activity was measured on a luminometer with automated injection of substrates. (**B**) Top: Overview of Foxp3-promoter vector with Promega pGL3 Luciferase reporter. Below: constructs with small *Foxp3* promoter sequences (500 bp) were cloned from the larger construct. (**C**) Transfection of HEK293 cells with *GFP*-transgene (left) or *Nr4a1* transgene (right) with a basic Luciferase reporter vector (Basic), a *Foxp3*-Fra1 reporter vector (Fra1) or the full *Foxp3* promoter vector (Full). X-axis vector, y-axis light units (Luciferase). (**D**) Co-transfection of HEK293 cells with either *Pcbp1*, *Sf1* or control (*GFP*) transgene, a *Foxp3* Luciferase vector and β-galactosidase normalization vector. X-axis indicates transgene and vector type, y-axis relative expression normalized to basic vector background. Statistical analysis with unpaired t-test (n=8, *p<0.05). (**E**) Co-transfection of HEK293 cells with either *Znf574*, *Rfx1*, *Naa38* or control (*GFP*) transgene, a *Foxp3* Luciferase vector and β-galactosidase normalization vector. X-axis indicates transgene and vector type, y-axis relative expression normalized to basic vector background. Statistical analysis with unpaired t-test (n=8, *p<0.05 and ***p<0.001). (**F**) Transfection of HEK293 cells with all transgenes using the assay described in (A). Transgenes were co-transfected with either the basic vector, *Foxp3*-Fra1, *Foxp3*-Fra2, *Foxp3*-Fra3 or a full *Foxp3* promoter vector as explained above. In the table, p-value is reported (unpaired t test, n=8). Significant values are highlighted in red.

Figure S4

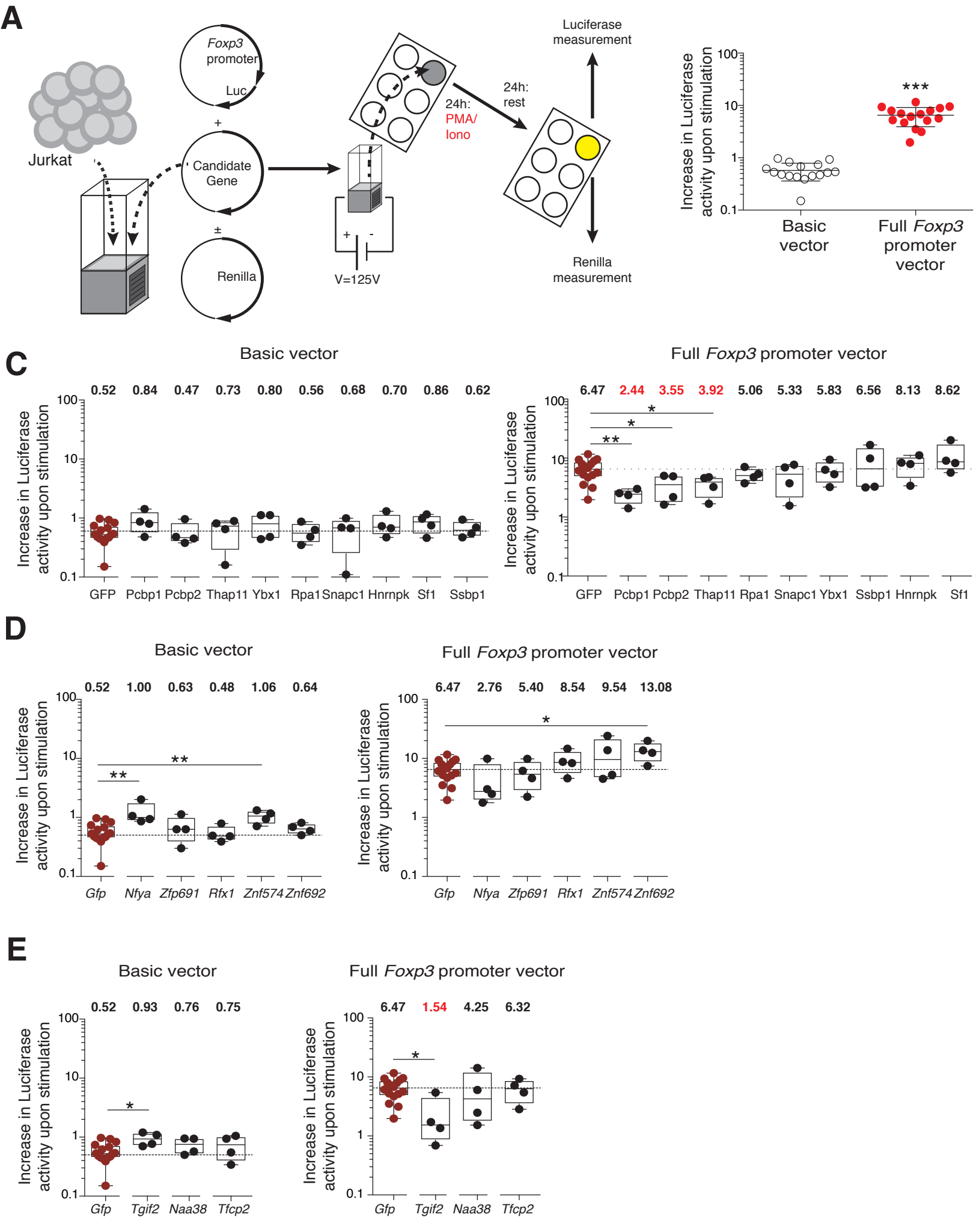
A
Jurkat
Foxp3 promoter
Luc
+
Candidate Gene
±
Renilla
+
-
V=125V
24h: PMA/ Iono
24h: rest
Luciferase measurement
Renilla measurement
B
Increase in Luciferase activity upon stimulation
100
10
1
0.1
***
Basic vector
Full Foxp3 promoter vector
C
Basic vector
Full Foxp3 promoter vector
Increase in Luciferase activity upon stimulation
0.52 0.84 0.47 0.73 0.80 0.56 0.68 0.70 0.86 0.62
GFP Pcbp1 Pcbp2 Thap11 Ybx1 Rpa1 Snapc1 Hnrnpk Sf1 Ssbp1
6.47 2.44 3.55 3.92 5.06 5.33 5.83 6.56 8.13 8.62
*
*
**
GFP Pcbp1 Pcbp2 Thap11 Rpa1 Snapc1 Ybx1 Ssbp1 Hnrnpk Sf1
D
Basic vector
Full Foxp3 promoter vector
Increase in Luciferase activity upon stimulation
0.52 1.00 0.63 0.48 1.06 0.64
**
**
Gfp Nfya Zfp691 Rfx1 Znf574 Znf692
6.47 2.76 5.40 8.54 9.54 13.08
*
Gfp Nfya Zfp691 Rfx1 Znf574 Znf692
E
Basic vector
Full Foxp3 promoter vector
Increase in Luciferase activity upon stimulation
0.52 0.93 0.76 0.75
*
Gfp Tgif2 Naa38 Tfcp2
6.47 1.54 4.25 6.32
*
Gfp Tgif2 Naa38 Tfcp2

Figure S4. Testing of candidate factors with *Foxp3*-Luciferase vectors in Jurkat cells, related to Figure 2 and Figure 3. (**A**) Experiment overview as in **Figure 3D**: 2,000,000 Jurkat cells were electroporated with a Renilla normalization vector, *Foxp3*-Luciferase reporter vector, and a eukaryotic expression vector containing the transgene of interest. 24h after electroporation, cells were stimulated with PMA/Ionomycin. 20h after stimulation, cells were lysed and Renilla as well as Luciferase enzyme activity was measured on a luminometer with automated injection of substrates. (**B**) Jurkat cells were electroporated with the basic vector containing no promoter in front of the Luciferase reporter and with the full *Foxp3* promoter vector. Luciferase reads were Renilla-normalized to adapt for electroporation efficiency changes. Then, normalized values were compared between unstimulated and stimulated conditions to calculate the increase in Luciferase activity upon stimulation (y-axis). Statistical analysis based on unpaired t test (n=16, ***p<0.001). (**C-E**) Jurkat cells were electroporated with either the full *Foxp3* promoter vector or the basic vector, with a Renilla normalization vector and the transgene vector of interest, as described above. Left, increase in Luciferase values upon stimulation with the basic vector, right with the full *Foxp3* promoter vector. Statistical evaluation based on unpaired t testing (n= 4-16, *p<0.05 and **p<0.01). Data are derived from four or more independent experiments.

Gene name	Direction	Sequence
Mouse Cux1	Forward	TGACCTGAGCGGTCCTTACA
Mouse Cux1	Reverse	TGGGGCCATGCCATTTACATC
Mouse Hnrnpab	Forward	ATGGCGGCTACGACTACTC
Mouse Hnrnpab	Reverse	GCTGGCTCTTTCCGTAATTTGT
Mouse Hnrnpd	Forward	GTGAAGTTGTAGACTGCACTCTG
Mouse Hnrnpd	Reverse	CCAAAACCCCTTGATCGCC
Mouse Hnrnpk	Forward	CAGCTCCCGCTCGAATCTG
Mouse Hnrnpk	Reverse	ACCCTATCAGGTTTTCCTCCAA
Mouse Naa38	Forward	GGCTGTTATTACTTCTGATGGCA
Mouse Naa38	Reverse	ACACCACTTGTTCTACTCCCT
Mouse Nfya	Forward	GTTAATGGTGCAAGTCAGTGGA
Mouse Nfya	Reverse	TCTGCTGTAAACCTTGTGTTCC
Mouse Pcbp1	Forward	GACGCCGGTGTGACTGAAA
Mouse Pcbp1	Reverse	GTCAGCGTGATGATCCTCTCC
Mouse Pcbp2	Forward	GCCAGATTTGACCAAGCTGC
Mouse Pcbp2	Reverse	GAGCTGGATTCAATGCCACTG
Mouse Rfx1	Forward	GTTCACGTTGCTCAAGAGGTA
Mouse Rfx1	Reverse	TACTGGTAGGTGCTAGAGCGG
Mouse Rfx1	Forward	AGTACCCGGAGACGCCTATC
Mouse Rfx1	Reverse	CTGCCGGACACATACATGG
Mouse Rpa1	Forward	ACATCCGTCCCATTTCTACAGG
Mouse Rpa1	Reverse	CTCCCTCGACCAGGGTGTT
Mouse Sf1	Forward	AGCCGATGGAACCAAGACAC
Mouse Sf1	Reverse	GCACTATGTAAGCTCTTTCCTGT
Mouse Sf1	Forward	AGAAGACCTGACTCGTAAACTGC
Mouse Sf1	Reverse	CCCTCGCTGTTGTAGATTGGT
Mouse Snapc1	Forward	CGCTTCCAAGAGATGGACAG
Mouse Snapc1	Reverse	CGTGTGTGGAGGCAAAAAGTAG
Mouse Ssbp1	Forward	CAACAAATGAGATGTGGCGATCA
Mouse Ssbp1	Reverse	ACGAGCTTCTTACCAGCTATGA
Mouse Tfcp2	Forward	TGAGTGATGTCCTCGCATTGC
Mouse Tfcp2	Reverse	TCGTTCTCATTATCGGGAGGC
Mouse Tgif2	Forward	ATGTCGGACAGCGATCTAGG
Mouse Tgif2	Reverse	TCCCGGAGGATCTTTACTGAC
Mouse Thap11	Forward	ATGCCTGGCTTTACGTGCT
Mouse Thap11	Reverse	GGTGGGTTGGAAGGTGGAG
Mouse Ybx1	Forward	CAGACCGTAACCATTATAGACGC
Mouse Ybx1	Reverse	ATCCCTCGTTCTTTTCCCCAC
Mouse Zfp574	Forward	ACATTGAGCACCGCTATGTCT
Mouse Zfp574	Reverse	CTCTCTTGGATGAGGGTCTGATA
Mouse Zfp691	Forward	GGAGAAGGGGCTAAACCTTGG
Mouse Zfp691	Reverse	GCAGTGACTTTCTGCCTTGTCT
Mouse Zfp691	Forward	GGAGAGTGGATGGCTCAAAGG
Mouse Zfp691	Reverse	CGTTCTCAGGTTGGAGGTATTGT
Mouse Zfp691	Forward	ATACCTCCAACCTGAGAACGC
Mouse Zfp691	Reverse	GGCGCATTGGTAGTGCTTC
Mouse Zfp692	Forward	GGTGCTCCTGTCTCACACAC
Mouse Zfp692	Reverse	CTGCTTAGGTACATCTGAAGGTG

Gene name	Direction	Sequence
Human Cux1	Forward	GAAGAACCAAGCCGAAACCAT
Human Cux1	Reverse	AGGCTCTGAACCTTATGCTCA
Human Foxp3	Forward	GTGGCCCGGATGTGAGAAG
Human Foxp3	Reverse	GGAGCCCTTGTCGGATGATG
Human Hnrnpab	Forward	ACCGAGAACGGACATGAGG
Human Hnrnpab	Reverse	GCCACCAACGAACATTTTTCC
Human Hnrnpd	Forward	GCGTGGGTTCTGCTTTATTACC
Human Hnrnpd	Reverse	TTGCTGATATTGTTCCTTCGACA
Human Hnrnpk	Forward	CAATGGTGAATTTGGTAAACGCC
Human Hnrnpk	Reverse	GTAGTCTGTACGGAGAGCCTTA
Human Hnrnpk	Forward	GCAGGAGGAATTATTGGGGTC
Human Hnrnpk	Reverse	TGCACTCTACAACCCTATCGG
Human Naa38	Forward	GCATTCGCATGACAGATGGAC
Human Naa38	Reverse	CGACGGCTTGAGGAACTCC
Human Nfya	Forward	CAGTGGAGGCCAGCTAATCAC
Human Nfya	Reverse	CCAGGTGGGACCAACTGTATT
Human Nfya	Forward	TGAAGGGCAGACCATCGTCTA
Human Nfya	Reverse	TCCTGTTTGAACAATCTGTGCT
Human Pcbp1	Forward	GCCGGTGTGACTGAAAGTG
Human Pcbp1	Reverse	CCCAATGATGCTTCCTACTTCC
Human Pcbp1	Forward	AAGAAAGGGGAGTCGGTTAAGA
Human Pcbp1	Reverse	GCCGGTCAGAGTGATGATTCTC
Human Pcbp2	Forward	ACTCTCACCATCCGGCTACTT
Human Pcbp2	Reverse	TCGCGCATCTTCTTAACTGATTC
Human Pcbp2	Forward	GCGCAGATCAAAATTGCGAAC
Human Pcbp2	Reverse	ATATTGAGCCAGGCTAATGCTG
Human Rfx1	Forward	CGTGGCTCAAGAGGTGCAG
Human Rfx1	Reverse	TCTCGGGATAGGAGTAGGTGC
Human Rfx1	Forward	CGGCAAGCACCAGCTACTAC
Human Rfx1	Reverse	GGACACGTACATGGGCATGG
Human Rpa1	Forward	GGGGATACAAACATAAAGCCCA
Human Rpa1	Reverse	CGATAACGCGGCGGACTATT
Human Rpa1	Forward	CGGGAATGGGTTCTACTGTTTC
Human Rpa1	Reverse	CGAGCACAAATGGTCCACTTG
Human Sf1	Forward	GAAGACCTGACTCGTAAACTGC
Human Sf1	Reverse	CCTCGCTATTGTAGATGGGCT
Human Sf1	Forward	GGAGCGGCACAACCTCATC
Human Sf1	Reverse	CCGGATCATAATCTTGGCATTGC
Human Snapc1	Forward	CGGACAGTGTACGCTTCGAG
Human Snapc1	Reverse	ATCGCCAAGCCAAAGCTAAAG
Human Snapc1	Forward	AGAGTTGGTGCTTTGTATCTGC
Human Snapc1	Reverse	GCTCTGTCTAGTCGTAGCTTCC
Human Ssbp1	Forward	TGAGTCCGAAACAACTACCAGT
Human Ssbp1	Reverse	CCTGATCGCCACATCTCATTAG
Human Ssbp1	Forward	ACTGGGTGATGTCAGTCAAAAG
Human Ssbp1	Reverse	TGCTTGTCGCCTCACATTATT
Human Tfcp2	Forward	TCTGGCCGACGAAGTGATTG
Human Tfcp2	Reverse	ATCAGGAGGCAAACTCGACTC
Human Tfcp2	Forward	GTGTTCCATGACAGAAGGCTT
Human Tfcp2	Reverse	TTATACCCACAGACATCGGGAT
Human Tgif2	Forward	TGACCCCTGGTAGCACACTTA
Human Tgif2	Reverse	GTGGTGGCGTGTTGAAGAGT

Human Thap11	Forward	ATGCCTGGCTTTACGTGCT
Human Thap11	Reverse	GCGTCCTTTGGAAACGTGTAG
Human Thap11	Forward	ATACTGGCTCCGACCATTCG
Human Thap11	Reverse	CTTGGCCTCAGTGAGACGC
Human Ybx1	Forward	GGGGACAAGAAGGTCATCGC
Human Ybx1	Reverse	CGAAGGTACTTCCTGGGGTTA
Human Ybx1	Forward	CCCCAGGAAGTACCTTCGC
Human Ybx1	Reverse	AGCGTCTATAATGGTTACGGTCT
Human Zfp574	Forward	ACATTGAGCACCGCTATGTCT
Human Zfp574	Reverse	CCTGCACAAGGGTCTGATAGA
Human Zfp574	Forward	AGACCCTTGTGCAGGAGAG
Human Zfp574	Reverse	GTGGTGCCTTAGGTGATGGC
Human Zfp691	Forward	GAGCAGAGTCCAGAACCACAC
Human Zfp691	Reverse	GCAGTTCATCCGACAGGCT
Human Zfp691	Forward	TCGGATGAACTGCAAGAAACTC
Human Zfp691	Reverse	TGTGTTCTCAGGTTGGAGGTA
Human Zfp692	Forward	TTCCGCACTAGCAGCAACC
Human Zfp692	Reverse	AAACCCGCATATCTCACACTG
Human Zfp692	Forward	TGTGAGATATGCGGGTTTACCT
Human Zfp692	Reverse	TGACTCTTGAGGGGCTAGAAG

Table S1. Sequences of qPCR primers for mouse and human genes, related to Figure 2.

TRANSPARENT METHODS

Ethics statement

Peripheral blood mononuclear cells for CD4 T-cell enrichment were isolated from leukocyte reduction chambers. Collection of blood cells from healthy donors was performed in compliance with the Helsinki Declaration. All donors signed an informed consent. The leukapheresis procedure and subsequent purification of immune cells were approved by the local ethical committee (reference number 13-101-0240).

Mice / cell lines

Animals were housed under specific pathogen-free conditions at the RCI or the DKFZ, and the governmental committee for animal experimentation (Regierungspräsidium Karlsruhe, Germany for DKFZ Heidelberg or Regierungspräsidium Unterfranken, Würzburg for Regensburg) approved all animal experiments. All experiments were conducted in accordance with the relevant regulatory standards. In these experiments, we used both female and male adult (>8 weeks of age) wild type C57/BL6 mice or Foxp3$^{GFP,\ DTR,\ CD45.1}$ C57/BL6 mice (Kim et al., 2007). TCF1-deficient animals were a received from Hans Clevers (Tcf7^{tm1Cle,} (Castrop et al., 1995; Verbeek et al., 1995)). For cell lines, we used a human embryonic kidney cell line (ATCC® CRL-1573™ and ATCC® CRL-3214™), a murine EL4 T-cell line (ATCC® TIB-39™), and a human Jurkat JE6.1 T-cell line (ATCC® TIB-152™). Cells were incubated at standard TC conditions (37°C, 5% CO2) in complete medium and were regularly tested for mycoplasma infection and contamination with other cell types.

Isolation of nuclear protein

Nuclear protein was isolated from EL4 T cells with the NXtract isolation kit (Sigma-Aldrich), and protein concentration was measured using a BCA kit (Thermo-Fisher #23225). Upon isolation of nuclear protein, a selective enrichment of nuclear protein of 5.5-fold compared to the cytosolic fraction as well as enrichment for nucleus-associated proteins based on gene ontology of detected peptides was achieved. About 40 mg of nuclear protein were used for each replicate.

Preparation of *Foxp3* Fra1, Fra2, and Fra3 probes

Short *Foxp3*-promoter fragments were produced from a Full *Foxp3* promoter vector with a biotinylated forward primer and standard reverse primers. PCR conditions for the production of biotinylated PCR primers were optimized to reduce a contamination with unbound biotinylated PCR primers. PCR products were purified using a quick PCR purification kit (Life Technologies #K3100-01). To measure biotinylation of the probe, the PCR product and its individual primers were plotted onto a PVDF membrane and UV cross-linked. Biotinylation was identified with an anti-biotin HRP and chromogenic detection.

Quantitative proteomics with *Foxp3* promoter DNA probes

The procedure is visualized in **Figure 1B** and described in literature (Mittler et al., 2009). First, carefully washed streptavidin beads were linked individually to *Foxp3*-Fra1 probes, *Foxp3*-Fra 2 probes, or *Foxp3*-Fra 3 probes for 3 hours at RT. Then, free bead binding sites were blocked and beads were washed again. Nuclear protein was pre-incubated with unlabeled beads to remove non-specific bead-binding proteins. The cleared nuclear

protein was then added to each probe-labeled bead and incubated on a rotating wheel for 3 hours at 4°C. After incubation, beads were washed to remove unbound protein and bead-bound sequence-specific proteins were eluted. Protein was trypsin-digested and peptides were labeled with stable isotopes by dimethylation of N-termini and lysines. Samples were then combined and reduced by isoelectric focusing. Finally, samples were subjected to nanoLC-MS analysis, which allows the quantitative detection of peptides that were originally bound to specific probe-labeled beads.

Real-time PCR to verify expression levels of candidate proteins

First, we synthesized and tested Sybr primers for both mouse and human candidate proteins with the aid of a public database (http://pga.mgh.harvard.edu/primerbank/). Primer efficiency and melting curve characteristics were analyzed, with efficiencies between 80% and 120% and single melting curves as criteria. We then isolated RNA from cell lines, FACS-sorted primary T_{reg} and T_{conv} cells or plasmid-transfected 293 cells with the RNeasy mini kit. RNA was concentration-adjusted and reversely transcribed using Reverse Transcriptase II and oligo(dT) primers (Life Technologies) according to manufacturer's standards. Real-time PCR was performed with Sybr Master Mix (Applied Biosystems) and Sybr primers. Sybr primer sequences are listed in **Table S1**.

Cloning of candidate genes and evaluation of proper expression for downstream reporter assays

First, we generated PCR products containing intron-free coding DNA for each candidate protein, either from mouse splenic cDNA or commercially available vector clones. PCR products were ligated into pENTR/D-TOPO® vectors (Life Technologies) and sequenced

for proper gene orientation and exclusion of mutations. Once complete, pENTR® vectors were used to shuttle coding DNA into destination vectors such as pDEST26® for eukaryotic overexpression and pMSCV-CD90.1® for viral transduction of T cells with LR clonase II enzyme (Life Technologies). Vectors were sequence-verified to exclude mutations. To exclude vector mix-ups and demonstrate eukaryotic expression, we transfected HEK293 cells with each pDEST® eukaryotic production vector and isolated RNA 48hrs post transfection followed by reverse transcription and real-time PCR. To verify transgene protein expression, we re-shuttled some pENTR®-based genes into FLAG®-tagged pDEST® eukaryotic production vectors and performed Western-Blot based detection of FLAG®-tagged protein with an anti-FLAG® antibody. Size and band intensity were used to identify the transgene of interest. Finally, we validated vector DNA integrity on agarose gels to ensure vector stability and concentration for downstream analyses.

Molecular cloning of short *Foxp3* promoter luciferase vectors

We used a full *Foxp3* promoter luciferase vector (Sekiya et al., 2011) as a template to create short *Foxp3* promoter Fragment 1, Fragment 2 and Fragment 3 PCR products with gene-specific primers including restriction-enzyme binding sites: *Foxp3* Fra 1 (ForP with *Xho*I CTAGCTCGAGACTGCTAGAGGGGGATCAGC and RevP with *Sbf*1 GATCCCTGCAGGGCAGGCTTCAGATCCCTTCT), *Foxp3* Fra 2 (ForP with *Xho*I CTAGCTCGAGCTGCCATGTGAATGGGAAG and RevP with *Sbf*1 GATCCCTGCAGGCCTGGGCCGCTATGTGTAT) and *Foxp3* Fra 3 (ForP with *Xho*I CTAGCTCGAGCCAGGGTCCTAGTCCTGTCA and RevP with *Sbf*1 GATCCCTGCAGGGTTGGCTTCAGGAAAACTGG). The Full *Foxp3* promoter vector was then digested with *Xho*I and *Sbf*1 restriction enzymes to remove the *Foxp3* promoter

sequence, size-separated and isolated from an agarose gel, and treated with phosphatase to prevent re-ligation. Next, the individual small fragments 1,2, or 3 were ligated into the empty vector. The *Foxp3* Fra1, Fra2, and Fra3-pGL3 vectors were sequenced to confirm proper orientation of the small *Foxp3* fragments into the luciferase reporter vector pGL3. All vector sequences and a vector map are supplied in the source data file.

Luciferase-based reporter assays in HEK 293 cells

First, we optimized the dual luciferase reporter system for cell seeding numbers, incubation time, linearity of the luciferase system, and transfection efficiencies. In our optimized protocol, we seeded 50,000 HEK 293 cells into a 96-well flat bottom plate on day 1. After overnight cell attachment, we added 125 ng each of three vectors: first, the β-galactosidase (β-gal) transfection normalization vector; second, a luciferase reporter vector, either the Full, Fra1, Fra2, or Fra3 *Foxp3* promoter vector; third, we added the transgene of interested in a eukaryotic production vector. A total of 375 ng of plasmid DNA were transfected into each well. For transfection, we used the Lipofectamine® transfection system (Life Technologies) according to manufacturer's recommendation. In short, the DNA-water mix containing all three vectors was mixed with a Lipofectamine®-medium suspension and incubated for 5 minutes at RT for liposome formation. Then, the liposomal mix was added to the cell culture and incubated for 24 hours. 50% of medium was exchanged followed by an additional 24 hours of incubation. 48 hours after transfection, cell culture medium was aspirated and cells were lysed with respective lysis buffer from a Dual Light luciferase kit (Thermo Fisher). 75 µL of supernatant were transferred to a black 96-well plate and 12.5 µL of buffer A was added. We then automatically injected 50 µL of

Buffer B plus X-GAL substrate and measured luciferase signals for the pGL3 luciferase vector on a luminometer (Berthold). After sixty minutes, another 50 µL of Accelerator-II solution were injected and the b-galactosidase signal was measured.

Normalization of luciferase values

To normalize transfection efficiency differences, we averaged β-gal light intensity values across all transfected wells of a 96-well plate. We then divided the β-gal readings of each individual well by the average β-gal intensity to determine a relative transfection efficiency reading. The measured luciferase values were then corrected for transfection differences by normalization with the respective β-gal ratio for each individual well.

$$\text{Transfection efficiency A1} = \frac{\text{Individual read (β-gal) A1}}{\text{Average (β-gal) across 96w plate}}$$

$$\text{Normalized luciferase A1} = \frac{\text{Individual read (luciferase) A1}}{\text{Transfection efficiency A1}}$$

Calculation of specific binding

To test for unspecific binding effects to elements on the pGL3 luciferase vector other than the integrated *Foxp3* promoter, we measured all our candidate proteins against a control-pGL3 vector, which does not contain any relevant promoter sequence before the luciferase ORF. We then cross-compared the normalized luciferase values for the Full *Foxp3* promoter vector as well as Fra1, Fra2 and Fra3 *Foxp3* promoter vectors against the control pGL3 vector to determine sequence-specific up-or downregulation of gene expression. To measure whether any of our candidate proteins significantly up-or downregulate *Foxp3* promoter activity, we compared normalized luciferase expression

values between cells co-transfected with GFP, a non-nuclear protein without transcription factor activity, and cells co-transfected with a candidate *Foxp3*-promoter binding protein.

$$\text{Sequence-specific binding} = \frac{\text{Norm. luciferase value for Foxp3-luciferase vector A2}}{\text{Norm. luciferase value for control-luciferase vector A1}}$$

Significance level for protein X = t.test (Specific binding GFP vs. Specific binding X)

Luciferase-based reporter assays in TCR-stimulated Jurkat cells

Analogously to the screenings described above, we used a three-vector system to check the effects of our candidate proteins in Jurkat T cells: The first vector was a luciferase reporter vector containing the Full *Foxp3* promoter sequence (5000 ng per test); the second vector was a eukaryotic production vector carrying the candidate gene (5000 ng per test); third, we used a Renilla-based normalization vector (500 ng per test). Before electroporation, Jurkat T cells were counted and adjusted to $2x10^6$ cells per electroporation. Cells were washed with OptiMEM medium and a mix of all three plasmids was added to each Jurkat cell preparation. Cells were transferred to electroporation cuvettes (Biorad) and electroporated with 125 V of electric current and “Mammalian 11 – Jurkat” settings with a Biorad electroporation machine. Afterwards, cells were transferred into pre-warmed six-well plates with 1500 µL of complete medium. 24 hours after incubation, electroporated cells were either stimulated with PMA (100 ng/µL) and Ionomycin (1000 ng/µL) or left untreated. 20 hours after stimulation, cells were washed and resuspended in 330 µL 1X lysis buffer (Promega) and lysed for 15 minutes at RT. Lysate was transferred to black 96-well plates, with 120 µL of luciferase measurements and 30 µL for Renilla measurements. Luciferase substrate and Renilla substrate were

freshly prepared (details see Appendix) and 100 µL were injected followed by 10s reading time on a luminometer (Berthold).

Calculation of specific binding for the Jurkat T cell screening

Similar to our transfection efficiency calculation for the HEK293-cell based screenings, we first averaged the Renilla transfection control values across all Renilla-transfected and non-stimulated samples. We then divided the individual Renilla read per well by the average reading to yield a measure of electroporation efficiency for each well. It should be noted that we used electroporation efficiencies of unstimulated wells to normalize PMA/Ionomycin-treated samples, since PMA specifically induces activity on the Renilla vector and thereby causes false-positive results also in the luciferase channel.

$$\text{Electroporation efficiency A1} = \frac{\text{Individual read (Renilla) A1}}{\text{Average (Renilla) across experiment}}$$

$$\text{Normalized luciferase A1} = \frac{\text{Individual read (luciferase) A1}}{\text{Electroporation efficiency A1}}$$

Next, we calculated normalized luciferase values for wells carrying the Full *Foxp3* pGL3 luciferase vector plus a selected transgene and calculated the relative induction compared to non-stimulated controls. These values were combined across four independent experiments and used to check for significant down-regulators in comparison to GFP controls.

$$\text{Relative Induction (protein X)} = \frac{\text{Normalized luciferase of stimulated well protein X}}{\text{Normalized luciferase of unstimulated well protein X}}$$

Significance level for protein X = t.test (Rel. Induction GFP vs. Rel. Induction X)

Viral transduction of candidate genes into primary induced T_{reg} cells

Retrovirus in the pMSCV-CD90.1® system can be manufactured in PhxEco cells, a pCL-Eco (packaging plasmid) carrying variant of HEK 293 cells. Therefore, PhxEco cells were seeded on a gelatin matrix at 400,000 cells per well in a six well plate 24 hours before lipofection. To produce liposomal particles containing the viral transgene, we co-incubated 3000ng of vector DNA and 1000ng of additional pCL-Eco packaging plasmid with 12 µL of TransIT-293® transfection reagent (Mirus) for 20 minutes at RT. Liposomes were added to PhxEco-carrying six-well plates and incubated for an additional 16 hours. CD4 T cells were enriched from whole spleen using anti-mouse CD4 biotinylated antibody (Biolegend Clone RM4-5) and anti-biotin ultrapure microbeads (Miltenyi Biotec). Cells were purified using magnetic columns (Miltenyi Biotec). Cells were activated with anti-mouse CD3/28 microbeads (Miltenyi T_{reg} expansion kit mouse #130-095-925) *in-vitro*. We also added 50 ng/mL TGF-β to T-cell cultures to induce Foxp3 expression. Two days after cell seeding, we added viral supernatant carrying pMSCV® retrovirus with the transgenes of interest. T cells were transduced by six hours of incubation at 37°C. Afterwards, viral supernatant was removed and cells were incubated with fresh medium supplemented with IL-2 and TGF-β for another 72 hours. Then, cells were harvested and surface-stained with CD4, CD90.1 and a live/dead exclusion dye, followed by fixation and intracellular staining for Foxp3 protein expression. Cells were analyzed on a BD CantoII™ or LSRII™ flow cytometer, and transduction efficiency was assessed by CD90.1 transgene expression level.

Viral transduction of candidate genes into primary T_{reg} cells

Virus was generated in PhxEco production cells. T_{reg} cells were isolated from murine spleens via bead-based pre-enrichment and FACS-based sorting of $CD4^+CD25^+Foxp3(GFP)^+$ T_{reg} cells on ARIAII™ or ARIAIII™ high-speed cell-sorting systems. T_{reg} cells were supplemented with high-dose IL-2 (2000 U/mL) and anti CD3-CD28 microbeads (Miltenyi T_{reg} expansion kit mouse #130-095-925). 48hrs after stimulation, T_{reg} cells were virally transduced as described above. 72hrs after viral transduction, T_{reg} cells were harvested and surface-stained with CD4, CD90.1 and a live/dead exclusion dye, followed by fixation and intracellular staining for Foxp3 protein expression. Cells were analyzed on a BD CantoII™ or LSRII™ flow cytometer, and transduction efficiency was assessed using CD90.1 transgene expression level.

CRISPR/Cas9-mediated deletion of TCF1 in mouse T cells

CD4 T cells were enriched from whole spleen using anti-mouse CD4 biotinylated antibody (Biolegend Clone RM4-5) and anti-biotin ultrapure microbeads (Miltenyi Biotec). Cells were purified using magnetic columns (Miltenyi Biotec) and FACS. Cells were activated with anti-mouse CD3/28 microbeads (Miltenyi) and IL-2 (Novartis, Proleukin S, 500 units/ml) for 3 days *in-vitro*. To induce Foxp3, TGF-β (Peprotech 100-21) was added at different concentrations. Knock-down was performed with 1.5 µM Cas9 protein (IDT, Alt-R S.p. Cas9 nuclease V3, 1081061), 1.8 µM tracrRNA (Alt-R CRISPR-Cas9 tracrRNA, 224102825), 1.8 µM *Tcf7* AC crRNA (3068068) or CD5 crRNA (2997292), 1.8 µM electroporation enhancer (Alt-R Cas9 electroporation enhancer) and 300,000 cells per transfection. Transfection was performed using the NEON transfection instrument (ThermoFisher, settings: 1600V, 10ms pulse width, 3 pulses). After electroporation cells

were cultured for 3-4 days at 37°C with anti-mouse CD3/28 microbeads and IL-2 (Novartis, Proleukin S, 500 units/ml).

CRISPR/Cas9-mediated deletion of TCF1 in human T cells

Human peripheral blood was separated by Ficoll gradient centrifugation and pre-enriched with anti-human CD4 biotinylated antibody (Biolegend Clone OKT-4) and anti-biotin beads (Miltenyi Biotec). Cells were purified using magnetic columns (Miltenyi Biotec), followed by fluorescence-activated cell sorting (FACS) for $CD4^+CD25^-CD127^+$ T_{conv}. Cells were activated with anti-human Transact (Miltenyi 130-111-160; 1µl/well) and IL-2 (Novartis, Proleukin S, 500 units/ml) for 3 days in serum-free medium (TexMACS™, Miltenyi Biotec #130-097-196). Knock-down was performed with 1.5 µM Cas9 protein (IDT, Alt-R S.p. Cas9 nuclease V3, 1081061), 1.8 µM tracrRNA (Alt-R CRISPR-Cas9 tracrRNA, 224102825), 1.8 µM *Tcf7* AA crRNA (299900012) or *Tcf7* AC crRNA (299900014), or control crRNA (224509651), 1.8 µM electroporation enhancer (Alt-R Cas9 electroporation enhancer) and 300,000 cells per transfection. Transfection was performed using the NEON transfection instrument (ThermoFisher, settings: 1600V, 10ms pulse width, 3 pulses). After electroporation cells were cultured for 4 days at 37°C with anti-human Transact and IL-2 (Novartis, Proleukin S, 500 units/ml).

CRISPR/Cas9-mediated deletion of TCF1 in human T cells followed by stimulation and intracellular cytokine secretion analysis

$CD4^+CD25^-CD127^+$ T_{conv} cells were sorted and human TCF1 was deleted as described above. Then, T cells were treated with a cell stimulation cocktail plus transport inhibitor (eBiosciences # 00-4975-03) for 4 hours at 37°C. Afterwards, cells were stained for

intracellular cytokine expression with a PE-conjugated anti-human IL-2 antibody (MQ1-17H12) and the Foxp3 transcription factor buffer set (eBiosciences 00-5523-00).

Flow cytometry of T cells

Spleen, lymph node or thymus were cut into small pieces and mechanically mashed using filters and syringe plumbers. Red blood cells were lysed using commercially-available ACK lysis buffer. Murine cells were surface-stained for 20 minutes at 4°C with anti-CD4 (RM4-5), anti-CD8 (53-6.7), anti-CD25 (PC61), anti-CD90.1 (OX-7), anti-CTLA4 (UC10-4B9) and a fixable live/dead dye (eBiosciences 65-0865-18). Human cells were surface-stained for 20 minutes at 4°C with anti-CD4 (OKT-4) and a fixable live/dead dye (eBiosciences 65-0865-18). Cells were fixed and permeabilized using the Foxp3 transcription factor buffer set (eBiosciences 00-5523-00). Intracellular staining was performed for 60 minutes at RT with anti-mouse Foxp3 (JFK-16) or anti-human Foxp3 (206D) antibody at 1:100 dilution in Perm buffer. Anti-mouse/human Tcf1 antibody (C63D9) and staining was performed for 60 minutes at RT at 1:100 dilution in Perm buffer, followed by washing steps and secondary intracellular staining with 1:200 anti-rabbit AF647 antibody (Molecular Probes A21244). Samples were acquired on BD LSRII, BD CantoII or BD FortessaII flow cytometers.

REFERENCES

Castrop, J., Verbeek, S., Hofhuis, F., and Clevers, H. (1995). Circumvention of tolerance for the nuclear T cell protein TCF-1 by immunization of TCF-1 knock-out mice. Immunobiology *193*, 281-287.

Kim, J.M., Rasmussen, J.P., and Rudensky, A.Y. (2007). Regulatory T cells prevent catastrophic autoimmunity throughout the lifespan of mice. Nat Immunol *8*, 191-197.

Mittler, G., Butter, F., and Mann, M. (2009). A SILAC-based DNA protein interaction screen that identifies candidate binding proteins to functional DNA elements. Genome Res *19*, 284-293.

Sekiya, T., Kashiwagi, I., Inoue, N., Morita, R., Hori, S., Waldmann, H., Rudensky, A.Y., Ichinose, H., Metzger, D., Chambon, P., and Yoshimura, A. (2011). The nuclear orphan receptor Nr4a2 induces Foxp3 and regulates differentiation of CD4+ T cells. Nat Commun *2*, 269.

Verbeek, S., Izon, D., Hofhuis, F., Robanus-Maandag, E., te Riele, H., van de Wetering, M., Oosterwegel, M., Wilson, A., MacDonald, H.R., and Clevers, H. (1995). An HMG-box-containing T-cell factor required for thymocyte differentiation. Nature *374*, 70-74.